



OsFTIP1-Mediated Regulation of Florigen Transport in Rice Is Negatively Regulated by the Ubiquitin-Like Domain Kinase OsUbdK γ 4

Shiyong Song,^{a,1} Ying Chen,^{a,1} Lu Liu,^a Yanwen Wang,^a Shengjie Bao,^a Xuan Zhou,^a Zhi Wei Norman Teo,^a Chuanzao Mao,^b Yinbo Gan,^c and Hao Yu^{a,2}

^aDepartment of Biological Sciences and Temasek Life Sciences Laboratory, National University of Singapore, 117543, Singapore

^bCollege of Life Science, Zhejiang University, Hangzhou 310058, China

^cCollege of Agriculture and Biotechnology, Zhejiang University, Hangzhou 310058, China

ORCID IDs: 0000-0002-0068-4807 (S.S.); 0000-0003-1615-7494 (Y.C.); 0000-0001-5126-2180 (C.M.); 0000-0002-9778-8855 (H.Y.)

Flowering time is a critical agronomic trait that determines successful seed production and adaptation of crop plants. Photoperiodic control of this process in flowering plants is mediated by the long-distance mobile signal called florigen partly encoded by *FLOWERING LOCUS T (FT)* in *Arabidopsis thaliana* and its orthologs in other plant species. Despite the progress in understanding FT transport in the dicot model *Arabidopsis*, the mechanisms of florigen transport in monocots, which provide most of the biomass in agriculture, are unknown. Here, we show that rice FT-INTERACTING PROTEIN1 (OsFTIP1), a member of the family of multiple C2 domain and transmembrane region proteins (MCTPs) and the closest ortholog of *Arabidopsis* FTIP1, is required for export of RICE FLOWERING LOCUS T 1 (RFT1) from companion cells to sieve elements. This affects RFT1 movement to the shoot apical meristem and its regulation of rice flowering time under long days. We further reveal that a ubiquitin-like domain kinase γ 4, OsUbdK γ 4, interacts with OsFTIP1 and modulates its degradation in leaves through the 26S proteasome, which in turn affects RFT1 transport to the shoot apical meristem. Thus, dynamic modulation of OsFTIP1 abundance in leaves by a negative regulator OsUbdK γ 4 is integral to the role of OsFTIP1 in mediating RFT1 transport in rice and provides key evidence for a conserved role of FTIP1-like MCTPs in mediating florigen transport in flowering plants.

INTRODUCTION

The timing of the transition from vegetative to reproductive growth is crucial for reproductive success in flowering plants. This transition to flowering is an important agronomic trait that determines yield and adaptation to changing environment of economically important cereal crops, including rice (*Oryza sativa*). As an essential source of calories for much of the world's human population, rice is a facultative short-day (SD) plant, but eventually flowers under noninductive long-day (LD) conditions. Rice cultivars have been developed through continuous domestication and breeding to adapt to a broad range of climatic conditions, such as different photoperiods (Izawa, 2007; Song et al., 2015).

Investigation of photoperiodic control of flowering time or heading date in rice has suggested that the proteins encoded by *Heading date 3a (Hd3a)* and its closest homolog *RICE FLOWERING LOCUS T1 (RFT1)*, both of which are rice orthologs of *Arabidopsis thaliana* *FLOWERING LOCUS T (FT)*, are part of the long-sought florigen that are essential for rice flowering (Corbesier et al., 2007; Jaeger and Wigge, 2007; Mathieu et al., 2007; Tamaki et al., 2007; Komiya et al., 2008). Knockdown of both *Hd3a* and

RFT1 in rice by RNA interference almost completely blocks flowering even under favorable SD conditions (Komiya et al., 2008). *Hd3a* and *RFT1* are diurnally expressed in leaves under SDs and LDs, and their proteins move to the shoot apical meristem (SAM), where they interact with a bZIP transcription factor OsFD to regulate the expression of two rice orthologs (*OsMADS14* and *OsMADS15*) of an *Arabidopsis* floral meristem identity gene *APETALA1*, thus provoking initiation of primary panicle branch primordia (Tamaki et al., 2007; Komiya et al., 2008, 2009; Taoka et al., 2011).

In the facultative LD model plant *Arabidopsis*, loss of function of *FT* and its homologs, such as *TWIN SISTER OF FT*, results in delayed flowering only under LDs (Kardailsky et al., 1999; Kobayashi et al., 1999; Yamaguchi et al., 2005; Jang et al., 2009), suggesting that *FT*-like genes are major determinants for the flowering response to LDs in *Arabidopsis*. By contrast, knockdown of *Hd3a* or *RFT1* in the *japonica* rice cultivar Norin 8 delays rice flowering only under SDs or LDs, respectively (Komiya et al., 2008, 2009), indicating that *Hd3a* and *RFT1* might be specific florigen in rice under SD and LD conditions, respectively. Analysis of *Hd3a* and *RFT1* nucleotide sequences in different rice cultivars has revealed that *RFT1* diverges more rapidly than *Hd3a* during the rice breeding process and that *RFT1* could have evolved with a specific florigen function under LDs for adapting to the photoperiodic conditions in many regions, such as north Asia, where rice is typically cultivated under LD conditions (Hagiwara et al., 2009). Interestingly, although mRNA expression of *Hd3a* and *RFT1* simultaneously increases during the floral transition under LDs,

¹ These authors contributed equally to this work.

² Address correspondence to dbsyuhao@nus.edu.sg.

The author responsible for distribution of materials integral to the findings presented in this article in accordance with the policy described in the Instructions for Authors (www.plantcell.org) is: Hao Yu (dbsyuhao@nus.edu.sg).

www.plantcell.org/cgi/doi/10.1105/tpc.16.00728

only *RFT1* affects rice flowering in response to this photoperiodic condition (Komiya et al., 2009), implying that the capacity of *Hd3a* and *RFT1* to affect flowering time under LDs might be modulated at the protein level.

Two Arabidopsis proteins, FT-INTERACTING PROTEIN1 (FTIP1) and SODIUM POTASSIUM ROOT DEFECTIVE1 (NaKR1), have been shown to regulate flowering time through mediating long-distance movement of FT from leaves to the SAM in response to LDs (Liu et al., 2012; Zhu et al., 2016). FTIP1 is a member of the family of multiple C2 domain and transmembrane region proteins (MCTPs) (Liu et al., 2013). It interacts with FT in companion cells of the phloem and specifically mediates FT protein movement from companion cells to sieve elements in the phloem (Liu et al., 2012). NaKR1, a heavy-metal-associated domain-containing protein, is activated by CONSTANS (CO) under LDs and regulates long-distance movement of FT and possibly other associated molecules required for flowering from sieve elements in leaves to those below the shoot apex (Tian et al., 2010; Zhu et al., 2016). Thus, FTIP1 and NaKR1 play sequential and additive roles in mediating FT transport from source leaves to the sink SAM through the phloem stream. However, despite the progress in exploring the mechanisms of FT transport in Arabidopsis, how florigen transport is mediated in other flowering plants, especially in economically important monocot plants, so far remains completely unknown.

To understand the underlying mechanisms of florigen transport in rice, we systematically investigated the biological functions of rice FTIP1-like MCTPs that contain three to four C2 domains at the N terminus and one to four transmembrane regions at the C terminus. In this study, we show that rice FTIP1 (OsFTIP1), the closest ortholog of Arabidopsis FTIP1, plays an essential role in mediating rice flowering time under LDs via its specific modulation on RFT1 transport from companion cells to sieve elements. This affects RFT1 movement to the SAM through the phloem stream and its further regulation of other genes involved in floral meristem development, such as *OsMADS14* and *OsMADS15*. We further show that a ubiquitin-like (UBL) domain kinase $\gamma 4$, OsUbdK $\gamma 4$, interacts with OsFTIP1 and mediates its degradation in leaves possibly through the ubiquitin-26S proteasome pathway. This regulates OsFTIP1 levels in leaves, which in turn affects RFT1 trafficking to the SAM, thus determining flowering time in rice under LDs. These results provide a mechanistic understanding of florigen transport in rice and reveal not only a conserved role of FTIP1-like MCTPs in mediating florigen transport in flowering plants, but also a hitherto unknown mechanism that dynamically regulates MCTP levels required for florigen transport in source tissues.

RESULTS

OsFTIP1 Regulates Flowering Time in Rice under LDs

To understand the biological role of 12 FTIP1-like MCTPs in rice, we systematically performed targeted mutagenesis of these genes in the Nipponbare cultivar background (*Oryza sativa* ssp *japonica*) using clustered regularly interspaced short palindromic repeats (CRISPR)/CRISPR-associated nuclease 9 (Cas9) technology (Feng et al., 2014). Among the rice mutants created, we observed delayed flowering phenotypes under LDs resulting from targeted mutations in *OsFTIP1* (Os06g0614000) (Figures 1A to

1E), a rice ortholog of Arabidopsis FTIP1 that contains three C2 domains and one phosphoribosyltransferase C-terminal domain (PRT_C) as shown in other FTIP1-like MCTPs (Supplemental Figure 1) (Liu et al., 2012, 2013). In the CRISPR/Cas9 system created for targeted mutagenesis of *OsFTIP1*, the single guide RNA (sgRNA) was designed to target the region 3' to the translational start site of *OsFTIP1* (Figure 1A). After genotyping and sequencing analysis of 80 T0 lines, we identified 10 independent lines that contained mutations (insertions or deletions) at 3 to 4 bp upstream of the protospacer adjacent motif, where the Cas9 cleavage site is located (Feng et al., 2014). After further sequencing targeted genomic regions of T2 populations derived from T1 homozygotes, we selected two homozygous mutants in the absence of the CRISPR/Cas9 transgene, *Osftip1-1* and *Osftip1-2*, which contained a 1-bp thymine (T) insertion and a 1-bp thymine (T) deletion, respectively (Figure 1A). Examination of the three most likely off-target sites of *OsFTIP1* in *Osftip1-1* and *Osftip1-2* did not reveal mutations in putative off-target loci (Supplemental Table 1), indicating that CRISPR/Cas9-mediated target mutagenesis of *OsFTIP1* is reliable and accurate.

Both *Osftip1-1* and *Osftip1-2* showed comparable flowering time to wild-type plants under SDs (Figures 1B and 1C) but flowered significantly later than wild-type plants under LDs (Figures 1D and 1E), suggesting that *OsFTIP1* plays a specific role in controlling rice flowering under LDs. We also created 15 *OsFTIP1* knockdown transgenic plants using RNA interference (RNAi), among which 11 lines exhibited different levels of late flowering under LDs. We measured *OsFTIP1* expression in six selected lines and found that the degrees of late flowering in *OsFTIP1* RNAi plants were mostly related to the levels of downregulation of *OsFTIP1* expression (Supplemental Figures 2A and 2B). In contrast, the expression of *Os05g0429700* and *Os04g0691800*, which shared the highest sequence similarity with *OsFTIP1* in the RNAi targeted region, was not obviously changed in these selected RNAi transgenic lines (Supplemental Figures 2C and 2D). These results, together with the flowering defect of *Osftip1* mutants, suggest that targeted disruption of *OsFTIP1* has a dosage-dependent effect on delaying flowering under LDs.

To confirm that the late-flowering phenotype of *Osftip1-1* is attributed to the loss of *OsFTIP1* function, we transformed *Osftip1-1* homozygous plants with a genomic construct (*gOsFTIP1*) harboring a 5.2-kb *OsFTIP1* genomic region including the 2.7-kb 5' upstream sequence and the entire 2.5-kb coding sequence (Supplemental Figure 3A). Among the independent lines regenerated, eight putative transformants containing the single-copy transgene were selected based on a 3:1 Mendelian segregation ratio by germination on hygromycin-containing media. Examination of their homozygous progenies at the T2 generation revealed that the late-flowering phenotype of *Osftip1-1* was rescued to different extents in these eight lines, among which six lines displayed comparable flowering time to wild-type plants (Supplemental Figure 3B), demonstrating that *OsFTIP1* is indeed responsible for the late-flowering phenotype observed in *Osftip1-1* under LDs.

Gene Expression and Subcellular Localization of OsFTIP1

We examined *OsFTIP1* expression in various tissues of wild-type plants using quantitative real-time PCR and found that *OsFTIP1*

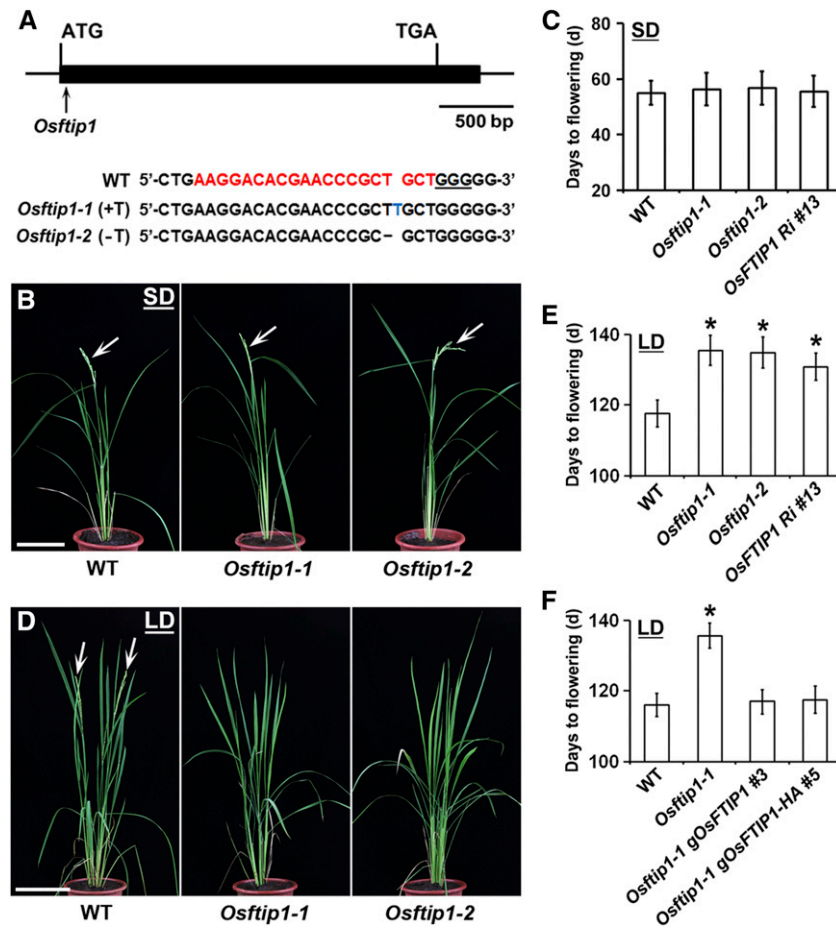


Figure 1. *OsFTIP1* Promotes Flowering in Rice under LDs.

(A) CRISPR/Cas9-mediated target mutagenesis of *OsFTIP1*. The upper panel shows schematic diagram of the *OsFTIP1* gene bearing the CRISPR/Cas9 target site indicated by an arrow. The exon and other genomic regions are represented by a black box and lines, respectively. The lower panel shows the alignment of wild-type, *Osftip1-1*, and *Osftip1-2* sequences containing the CRISPR/Cas9 target site. A 20-bp CRISPR/Cas9 target sequence adjacent to the underlined protospacer adjacent motif is indicated in red in the wild-type sequence. The newly created *Osftip1-1* and *Osftip1-2* mutants contain a 1-bp insertion (T, blue font) and a 1-bp deletion (T, dash), respectively.

(B) *Osftip1-1* and *Osftip1-2* exhibit similar flowering time to a wild-type plant grown under SDs at 60 DAS. Arrows indicate panicles. Bar = 15 cm.

(C) Days to flowering of *Osftip1* mutants and representative RNAi transgenic plants (*OsFTIP1 Ri* line 13) under SDs. $n = 15$; error bars denote sd.

(D) *Osftip1-1* and *Osftip1-2* display later flowering than a wild-type plant grown at 120 DAS under LDs. Arrows indicate panicles. Bar = 15 cm.

(E) Days to flowering of *Osftip1* mutants and representative RNAi transgenic plants (*OsFTIP1 Ri* #13) under LDs. $n = 15$; error bars denote sd. Asterisks indicate significant differences in flowering time of *Osftip1-1*, *Osftip1-2*, and *OsFTIP1 Ri* #13 compared with that of wild-type plants (Student's t test, $P < 0.05$).

(F) Days to flowering of two representative *Osftip1-1* lines harboring *gOsFTIP1* and *gOsFTIP1-HA*, respectively, under LDs. $n = 12$; error bars denote sd. Asterisk indicates a significant difference in flowering time of *Osftip1-1* compared with that of wild-type and two rescued *Osftip1-1* plants (Student's t test, $P < 0.05$).

was ubiquitously expressed in all tissues examined with the highest expression in panicles and leaves (Figure 2A). In addition, *OsFTIP1* was expressed at comparable levels in leaves under LDs and SDs (Supplemental Figure 4A). To monitor the detailed tissue-specific expression pattern of *OsFTIP1*, we created a *ProOsFTIP1*: β -glucuronidase (*GUS*) reporter construct in which the same 2.7-kb 5' upstream sequence included in *gFTIP1* for the gene complementation test (Supplemental Figure 3A) was fused to the *GUS* reporter gene (Supplemental Figure 4B). Among the 12 independent *ProOsFTIP1*:*GUS* lines created, most lines showed similar *GUS* staining patterns. *ProOsFTIP1*:*GUS* exhibited specific *GUS*

staining in vascular tissues of various plant organs, including leaves (Supplemental Figures 4C to 4G). Examination of a transverse section of a *ProOsFTIP1*:*GUS* leaf revealed that *ProOsFTIP1*:*GUS* expression was specifically located in the phloem, including companion cells (Figure 2B, left panel), which is similar to the *FTIP1* expression pattern in Arabidopsis (Liu et al., 2012), indicating that *OsFTIP1* acts in the phloem to promote flowering.

We further examined the subcellular localization of *OsFTIP1* through transiently expressing *Pro35S*:*GFP-OsFTIP1* with various fluorescent protein-tagged organelle markers (Nelson et al., 2007) in *Nicotiana benthamiana* leaf epidermal cells and found that

GFP-OsFTIP1 colocalized with the RFP-tagged endoplasmic reticulum (ER) marker ER-RFP in whole cells (Figure 2C). In contrast to free GFP control, GFP-OsFTIP1 was not localized in the nucleus.

To precisely localize OsFTIP1 protein in the phloem in rice, we performed immunoelectron microscopy on an *Osftip1-1 gOsFTIP1-HA* transgenic line (#5), in which *gOsFTIP1-HA* was able to fully rescue the flowering defect of *Osftip1-1* (Figure 1F; Supplemental Figures 3B and 3C). Notably, OsFTIP1-HA signals, specifically detected by anti-HA antibody (Supplemental Figure 8A), were only found in phloem companion cells, but not in sieve elements (Figure 2D). This protein localization pattern is consistent with the *ProOsFTIP1:GUS* expression pattern (Figure 2B), implying that OsFTIP1 is synthesized and functional in companion cells. Unlike the localization of FTIP1 and its homolog QUIRKY in Arabidopsis plasmodesmata (Fulton et al., 2009; Liu et al., 2012; Vaddepalli et al., 2014), OsFTIP1-HA did not appear to be present in plasmodesmata between companion cells and sieve elements in rice. It is technically challenging to clearly identify plasmodesmata between companion cells and sieve elements by transmission electron microscopy in rice. On very few occasions when we could identify plasmodesmata between companion cells and sieve elements on the sections, we did not observe OsFTIP1-HA signals. This very small number of negative observations did not allow us to determine whether OsFTIP1-HA was localized to the plasmodesmata between companion cells and sieve elements, and this possibility remains to be resolved in rice.

OsFTIP1 Interacts with RFT1

To test whether the effect of *OsFTIP1* on rice flowering under LDs (Figure 1) is related to either *Hd3a* or *RFT1* in the Nipponbare cultivar background, we first generated *hd3a* and *rft1* mutants through CRISPR/Cas9-mediated target mutagenesis. Given that *Hd3a* and *RFT1* share high sequence similarity, sgRNAs were designed to target regions that exhibit relatively low sequence similarity between *Hd3a* and *RFT1* (Supplemental Figure 5A). We eventually created two homozygous mutants for either *Hd3a* or *RFT1* in the absence of the CRISPR/Cas9 transgene. There was an adenine (A) insertion and a cytosine (C) deletion in *hd3a-1* and *hd3a-2*, respectively, while *rft1-1* and *rft1-2* contained a thymine (T) insertion and a cytosine (C) deletion, respectively (Supplemental Figures 5B and 5C). All these mutations resulted in premature termination of Hd3a and RFT1 proteins with only around 50 to 60 amino acids. Examination of the three most likely off-target sites of *Hd3a* and *RFT1* in these mutants did not reveal any unexpected mutations in the putative off-target loci (Supplemental Table 1). In agreement with the observations on *Hd3a* and *RFT1* RNAi lines in the Norin 8 cultivar background (Komiya et al., 2009), *hd3a* or *rft1* mutants in the Nipponbare cultivar background also displayed late-flowering phenotypes only under SDs or LDs, respectively (Supplemental Figures 5D and 5E), substantiating that *Hd3a* and *RFT1* are specific florigen required for rice flowering under SDs and LDs, respectively.

As both *OsFTIP1* and *RFT1* affected rice flowering mainly under LDs (Figure 1), we proceeded to investigate their relationship by

comparing *GUS* expression patterns in leaf transverse sections of *ProOsFTIP1:GUS* and *ProRFT1:GUS* (Hayama et al., 2003) under LDs. *GUS* expression in both transgenic lines displayed a similar pattern in the phloem, including companion cells (Figure 2B). Furthermore, transient expression of *Pro35S:GFP-OsFTIP1* and *Pro35S:RFT1-RFP* in *N. benthamiana* leaf epidermal cells revealed colocalization of GFP-OsFTIP1 and RFT1-RFP in whole cells, including ER (Figure 3A; Supplemental Figure 6). Compared with GFP-OsFTIP1, RFT1-RFP was also localized in the nucleus (Figure 3A).

The similar tissue expression and subcellular localization of OsFTIP1 and RFT1 prompted us to carry out a detailed analysis of their potential protein interaction by different approaches. A yeast two-hybrid assay revealed the interaction of RFT1 with a truncated OsFTIP1 containing only three C2 domains at the N terminus, but not with the full-length OsFTIP1 (Figure 3B). This is consistent with the yeast two-hybrid result showing the interaction between FT and FTIP1 in Arabidopsis (Liu et al., 2012), implying that the PRT_C domain containing the transmembrane regions at the C termini of FTIP1-like MCTPs (Supplemental Figures 1A and 1B) may interfere with the interaction between FTIP1-like MCTPs and FT-like proteins in yeast cells. To determine which C2 domain is responsible for the interaction of OsFTIP1 with RFT1, we created a series of constructs containing various OsFTIP1 truncated proteins for further yeast two-hybrid assays (Figure 3C, left panel). The results showed that the truncated proteins bearing the third C2 domain consistently interacted with RFT1 (Figure 3C, right panel), indicating that this specific C2 domain is required for the interaction of OsFTIP1 with RFT1.

A glutathione S-transferase (GST) pull-down assay demonstrated that OsFTIP1-HA generated from rice protoplasts bound to in vitro-translated GST-RFT, but not GST (Figure 3D). Bimolecular fluorescence complementation (BiFC) experiments also revealed the enhanced YFP (EYFP) signal in *N. benthamiana* leaf epidermal cells except the nuclei (Figure 3E), implying a direct interaction between OsFTIP1 and RFT1 in living tobacco cells. To further test the in vivo interaction between OsFTIP1 and RFT1 in rice, we attempted to create *gRFT1-FLAG gOsFTIP1-HA* plants in which the transgenic alleles of *gRFT1-FLAG* (#2) and *gOsFTIP1-HA* (#5) were able to rescue *rft1-1* and *Osftip1-1*, respectively (Supplemental Figures 3B, 3C, 7A, and 7B). We transformed *rft1-1* with a genomic construct (*gRFT1-FLAG*) that contained a 4.4-kb *RFT1* genomic fragment including the 2-kb 5' upstream sequence and the 2.4-kb coding sequence plus introns (Komiya et al., 2009) fused in frame with a FLAG tag. The T2 homozygous progenies from three selected lines, which could harbor the single-copy transgene based on a 3:1 Mendelian segregation ratio, displayed significantly rescued flowering time compared with *rft1-1* under LDs (Supplemental Figure 7A). We selected the *rft1-1 gRFT1-FLAG* (#2) that exhibited comparable flowering time to wild-type plants (Supplemental Figures 7A and 7B) for further genetic crossing with plants in various genetic backgrounds, including *gOsFTIP1-HA* (#5) (Supplemental Figures 3B and 3C). Coimmunoprecipitation analysis of protein extracts from *gOsFTIP1-HA* and *gRFT1-FLAG gOsFTIP1-HA* plants confirmed the in vivo interaction of OsFTIP1-HA and RFT1-FLAG in *gRFT1-FLAG gOsFTIP1-HA* leaves under LDs (Figure 3F). Taken together, these

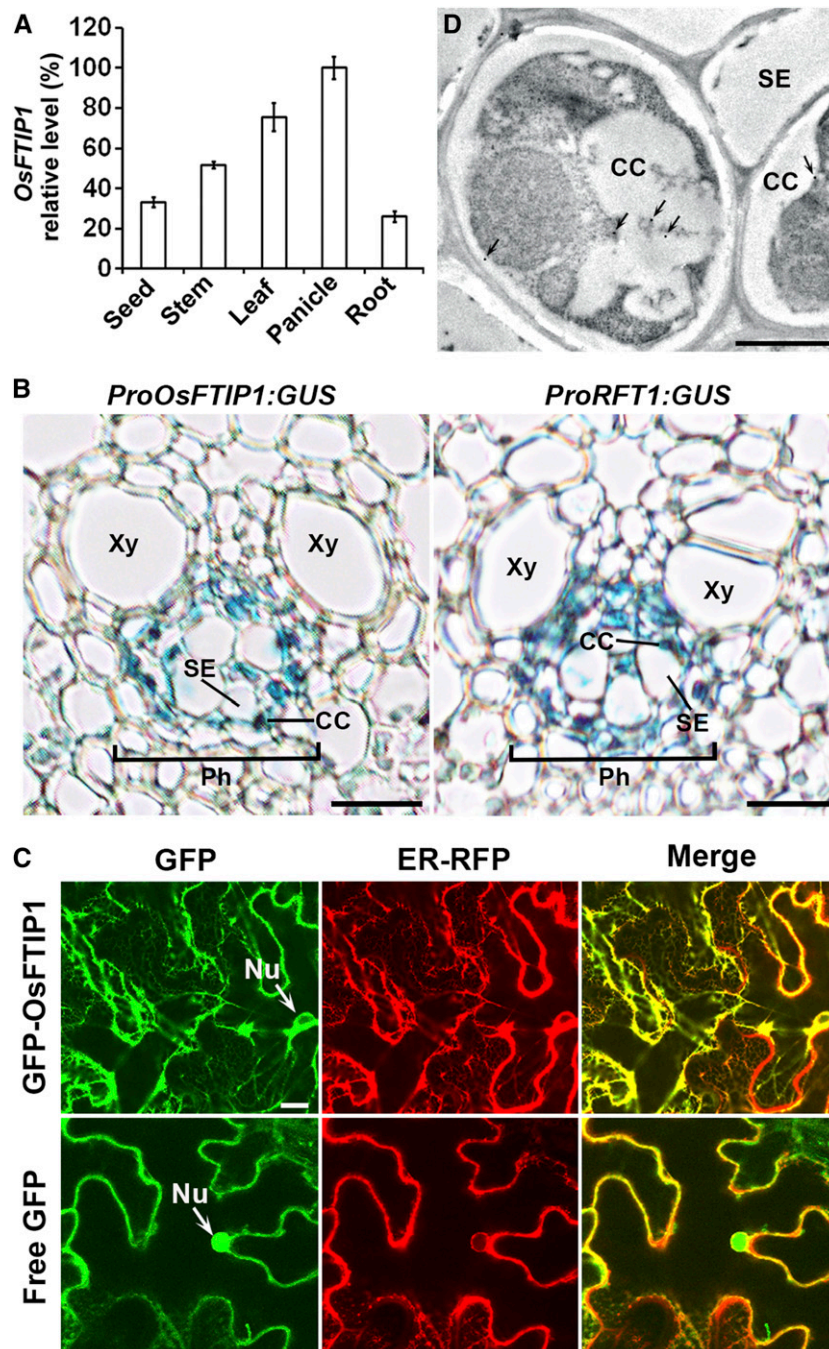


Figure 2. Expression Patterns of *OsFTIP1*.

(A) Quantitative real-time PCR analysis of *OsFTIP1* expression in various tissues of wild-type plants grown under LDs. Results were normalized against the expression levels of *Ubiquitin* based on three biological replicates. Error bars indicate *sd*.

(B) Transverse section of the leaf blade from representative *ProOsFTIP1:GUS* and *ProRFT1:GUS* transgenic plants grown under LDs at 50 DAS. CC, companion cell; Ph, phloem; SE, sieve element; Xy, xylem. Bars = 10 μ m.

(C) Subcellular localization of GFP-*OsFTIP1* and free GFP in *N. benthamiana* leaf epidermal cells. GFP-*OsFTIP1* is mostly colocalized with an ER marker. GFP, GFP fluorescence; ER-RFP, RFP fluorescence of an ER marker; Merge, merge of GFP and RFP; Nu, nucleus. Bar = 10 μ m.

(D) Analysis of *OsFTIP1*-HA localization by immunogold electron microscopy using anti-HA antibody in companion cell-sieve element complexes in the leaf vasculature of *Osftip1-1 gOsFTIP1-HA*. Arrows indicate the locations of gold particles. CC, companion cell; SE, sieve element. Bar = 1 μ m.

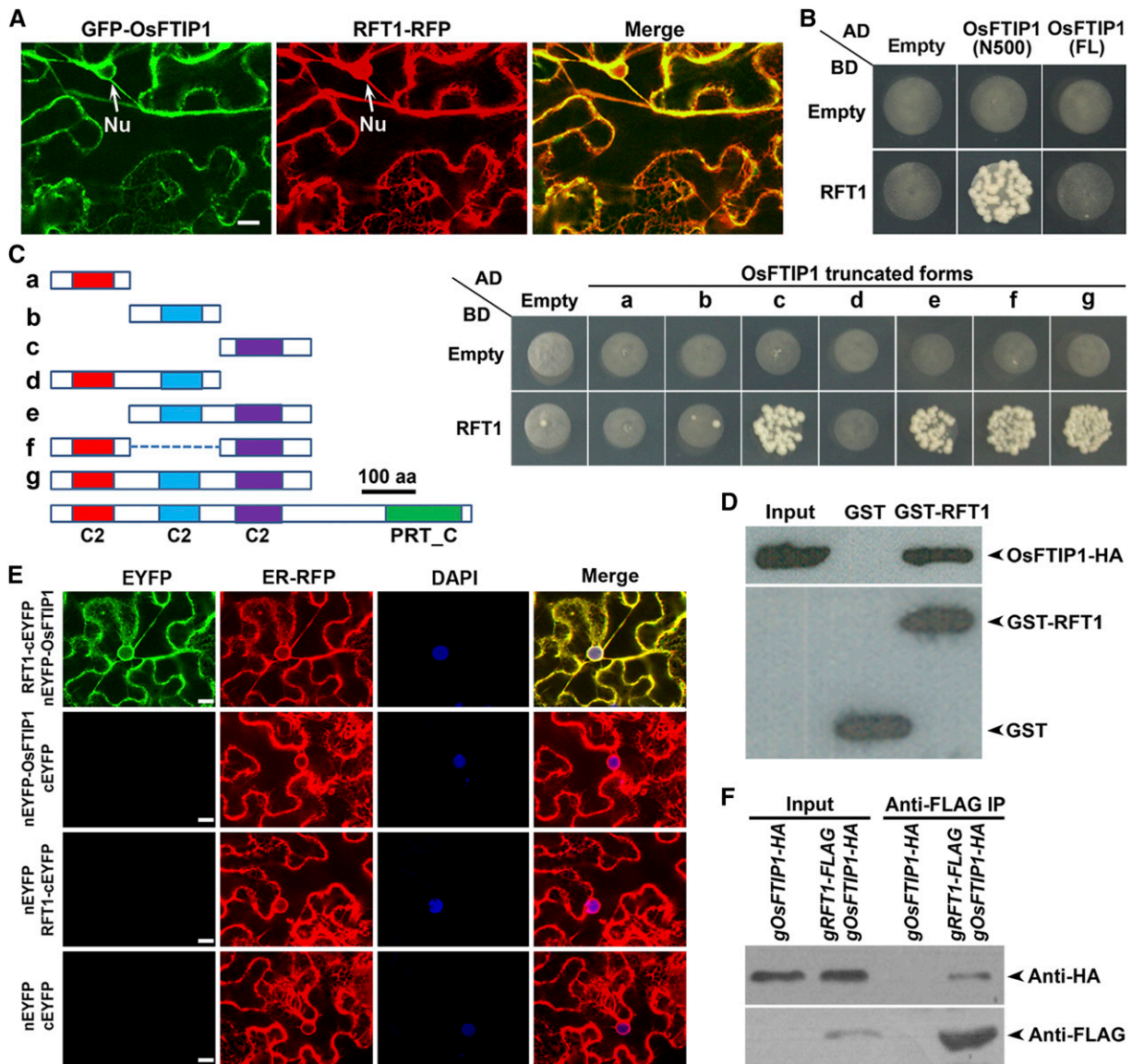


Figure 3. OsFTIP1 Interacts with RFT1.

(A) Colocalization of GFP-OsFTIP1 and RFT1-RFP in *N. benthamiana* leaf epidermal cells. Merge, merge of GFP and RFP images; Nu, nucleus. Bar = 20 μ m.

(B) Yeast two-hybrid assay of interaction between RFT1 and full-length OsFTIP1 (FL) and its N terminus (amino acids 1–500; N500) containing three C2 domains. Transformed yeast cells were grown on SD-His⁻Trp⁻Leu medium supplemented with 2 mM 3-amino-1,2,4-triazole. Empty refers to AD- or BD-containing vector only.

(C) Yeast two-hybrid assay evaluating interaction between RFT1 and various OsFTIP1 truncated proteins. The left panel shows schematic diagrams of OsFTIP1 truncated proteins (a–g) that were fused to AD. Full-length OsFTIP1 protein including three C2 domains and the PRT_C domain at the N and C termini, respectively, is presented at the bottom. The right panel shows the results of the yeast two-hybrid assay.

(D) In vitro GST pull-down assay evaluating interaction between RFT1 and OsFTIP1. HA-tagged OsFTIP1 generated from rice protoplasts was incubated with immobilized GST or GST-RFT1, respectively. Immunoblot analysis was performed using either anti-HA (upper panel) or anti-GST (lower panel) antibody. Input, 5% of the protein generated from rice protoplasts.

(E) BiFC analysis of interaction between RFT1 and OsFTIP1. DAPI, fluorescence of 4',6-diamino-2-phenylindole; Merge, merge of EYFP, RFP, and DAPI images. Bars = 10 μ m.

(F) In vivo interaction between OsFTIP1 and RFT1 shown by coimmunoprecipitation in rice. Total protein extracts from leaves of *gOsFTIP1-HA* and *gRFT1-FLAG gOsFTIP1-HA* plants grown at 50 DAS under LDs were immunoprecipitated by anti-FLAG beads. The input and coimmunoprecipitated protein were detected by either anti-HA (upper panel) or anti-FLAG (lower panel) antibody.

results suggest that OsFTIP1 interacts *in vivo* with RFT1 in rice leaves. Interestingly, as *Osftip1-1 rft1-1* flowered later than the respective single mutants (Figure 4A), both proteins may either interact to have a synergistic effect on rice flowering or act independently with other unknown coregulator(s) involved in the control of rice flowering time.

OsFTIP1 Affects RFT1 Transport from Leaves to the SAM

Given that OsFTIP1 and RFT1 interacted with each other *in vivo* and shared overlapping expression patterns at the tissue and subcellular levels, it is possible that OsFTIP1 controls rice flowering through mediating RFT1 function. To elucidate the biological significance of the interaction between OsFTIP1 and RFT1, we first examined how OsFTIP1 influences the effect of RFT1 on rice flowering using various genetically crossed materials containing the biologically functional *gRFT1-FLAG* allele (#2) (Supplemental Figures 7A and 7B). This *gRFT1-FLAG* allele fully rescued the late-flowering phenotype of *rft1-1* (Supplemental Figures 7A and 7B), and plants harboring this construct exhibited earlier flowering than wild-type plants under LDs because of higher levels of *RFT1* transcripts including both transgenic and endogenous *RFT1* expression (Supplemental Figure 7C).

Both *Osftip1-1* and *Osftip1-2* suppressed the early flowering phenotype of *gRFT1-FLAG*, while supply of OsFTIP1 activity in *Osftip1-1 gOsFTIP1* restored the promotive effect of *gRFT1-FLAG* on flowering (Figures 4B), indicating that the effect of RFT1 on rice flowering is partially dependent on OsFTIP1. We found that RFT1-FLAG protein levels, specifically detected by anti-FLAG antibody (Supplemental Figure 8A), were comparable in leaves of *gRFT1-FLAG* plants in various genetic backgrounds grown under LDs at 50 d after sowing (DAS), when these plants were undergoing the floral transition (Supplemental Figure 7D). However, the levels of RFT1-FLAG protein in the SAMs were lower in the *gRFT1-FLAG Osftip1-1* and *gRFT1-FLAG Osftip1-2* backgrounds than in the *gRFT1-FLAG* and *gRFT1-FLAG Osftip1-1 gOsFTIP1* backgrounds (Figure 4C; Supplemental Figure 12A). Consistently, the expression of *OsMADS14* and *OsMADS15*, which are involved in floral meristem development and activated by RFT1 in SAMs (Komiya et al., 2009), was downregulated in *gRFT1-FLAG Osftip1-1* but restored in *gRFT1-FLAG Osftip1-1 gOsFTIP1* (Figure 4D). Thus, the flowering phenotypes of *gRFT1-FLAG* plants in various genetic backgrounds are closely relevant to RFT1-FLAG protein levels in SAMs, which are downregulated in the absence of OsFTIP1.

RFT1 is synthesized in leaves and moves to the SAM through the phloem (Komiya et al., 2009). Since OsFTIP1 did not affect RFT1-FLAG levels in leaves (Supplemental Figure 7D), we hypothesized that the effect of OsFTIP1 on RFT1-FLAG abundance in SAMs might be due to modulation of RFT1-FLAG transport through the phloem. As OsFTIP1-HA signals were only present in phloem companion cells, but not in sieve elements (Figure 2D), we then examined whether OsFTIP1 affects RFT1 export from companion cells to sieve elements in *gRFT1-FLAG* lines in both wild-type and *Osftip1-1* backgrounds using immunoelectron microscopy (Figure 4E). RFT1-FLAG signals detected by anti-FLAG antibody were found in companion cells in both wild-type

and *Osftip1-1* backgrounds, albeit at different frequencies, whereas in sieve elements the signals were greatly reduced in the *Osftip1-1* background (Figure 4E, upper panel). Quantitative analysis of RFT1-FLAG signals in companion cell-sieve element complexes showed that although all sections from *gRFT1-FLAG* and *gRFT1-FLAG Osftip1-1* displayed RFT1-FLAG signals in companion cells (Figure 4E, lower right panel), there was an approximate 2.5-fold enrichment of signals in *Osftip1-1* over the wild-type background (Figure 4E, lower left panel). RFT1-FLAG signals appeared in sieve elements in nearly 75% of the wild-type sections, but only in 12% of the *Osftip1-1* sections (Figure 4E, lower right panel). Furthermore, RFT1-FLAG signals in sieve elements were much stronger in the wild type than in *Osftip1-1* (Figure 4E, lower left panel). Thus, RFT1-FLAG accumulates in companion cells and its transport to sieve elements is compromised when OsFTIP1 activity is impaired. In contrast, we found that OsFTIP1 did not affect localization of free FLAG in companion cell-sieve element complexes (Supplemental Figure 8B). These observations strongly suggest that OsFTIP1 specifically mediates RFT1 export from phloem companion cells to sieve elements, thus affecting RFT1 transport through the phloem to the SAM.

OsFTIP1 Interacts with OsUbDK γ 4

To further examine how OsFTIP1 activity is regulated, we performed yeast two-hybrid screening to identify putative interaction partners of the truncated OsFTIP1 bearing the N-terminal C2 domains (Supplemental Table 2). One of the interactors identified was a phosphatidylinositol 3-/4-kinase (PI3/4K) family protein (OsUbDK γ 4) containing two N-terminal UBL domains and a C-terminal PI3/4K domain (Supplemental Figure 9A). PI3/4K family proteins have been found to regulate diverse cellular functions, including lipid- and protein-mediated signaling pathways (Fruman et al., 1998; Balla and Balla, 2006). Interestingly, the Arabidopsis ortholog of OsUbDK γ 4, UbDK γ 4, has been suggested to facilitate substrate delivery to the 26S proteasome (Galvão et al., 2008). We then sought to investigate how OsUbDK γ 4 interacts with OsFTIP1 to modulate OsFTIP1 in rice. Yeast two-hybrid assay confirmed the interaction between OsUbDK γ 4 and the truncated OsFTIP1 devoid of the PRT_C domain, but not with the full-length OsFTIP1 (Figure 5A). GST pull-down assay demonstrated that OsFTIP1-HA generated from rice protoplasts bound to *in vitro*-translated GST-OsUbDK γ 4, but not GST (Figure 5B). To further investigate the *in planta* interaction between OsUbDK γ 4 and OsFTIP1, we co-transformed *Pro35S:OsUbDK γ 4-GFP* and *Pro35S:OsFTIP1-HA* into rice protoplasts. Coimmunoprecipitation analysis of the protein extracts revealed that OsUbDK γ 4-GFP interacted with OsFTIP1-HA only in the protoplasts transformed with both *Pro35S:OsUbDK γ 4-GFP* and *Pro35S:OsFTIP1-HA* (Figure 5C). These results all support the notion that OsFTIP1 interacts with OsUbDK γ 4.

We found that like *OsFTIP1*, *OsUbDK γ 4* was ubiquitously expressed in all tissues examined, with expression being highest in panicles and leaves (Figure 2A; Supplemental Figure 9B). We also created a *ProOsUbDK γ 4:GUS* reporter construct in which the same 3.1-kb *OsUbDK γ 4* 5' upstream sequence

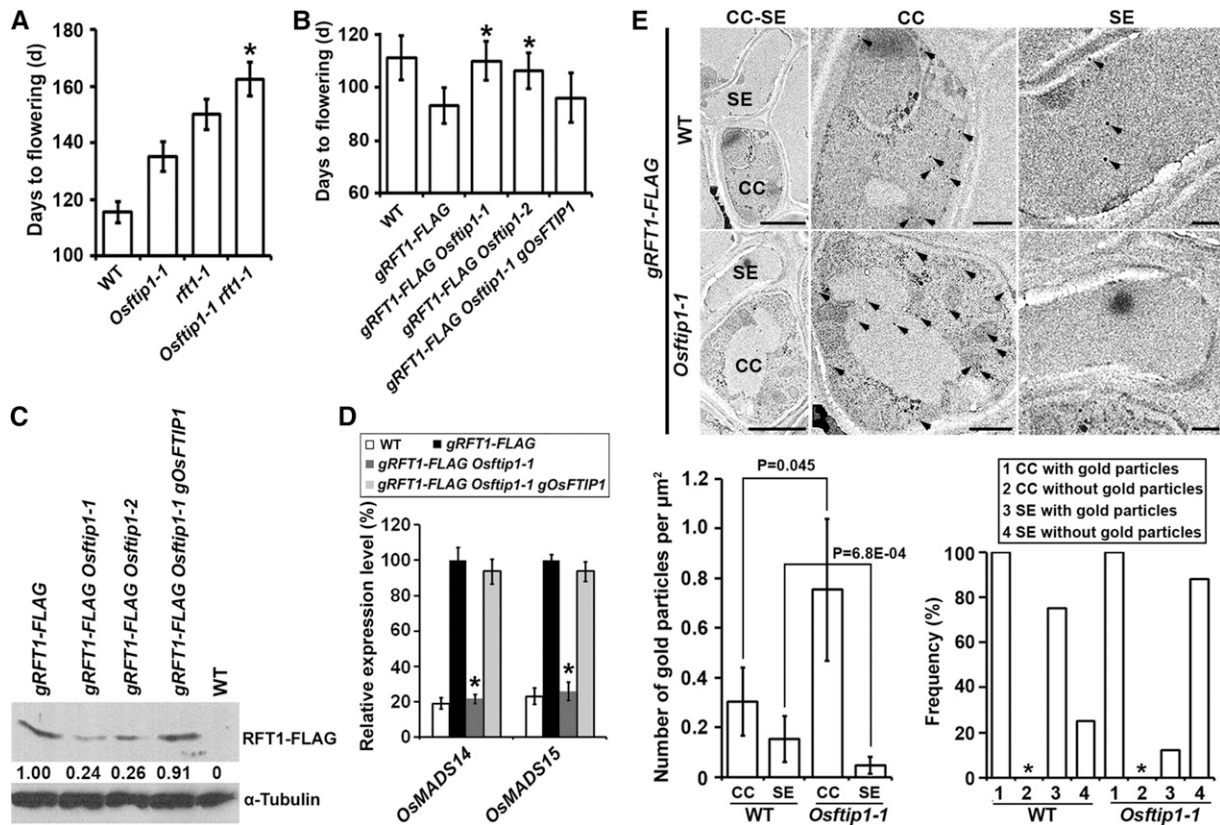


Figure 4. OsFTIP1 Affects RFT1 Transport.

(A) Days to flowering of *Osftip1-1 rft1-1* under LDs. $n = 15$; error bars denote sd. Asterisk indicates a significant difference in flowering time of *Osftip1-1 rft1-1* compared with that of *Osftip1-1* or *rft1-1* (Student's t test, $P < 0.05$).

(B) Days to flowering of *gRFT1-FLAG* plants in various genetic backgrounds under LDs. $n = 15$; error bars denote sd. Asterisks indicate significant differences in flowering time of *gRFT1-FLAG Osftip1-1* and *gRFT1-FLAG Osftip1-2* compared with that of *gRFT1-FLAG* (Student's t test, $P < 0.05$).

(C) Immunoblot analysis using anti-FLAG antibody shows RFT1-FLAG abundance in SAMs of *gRFT1-FLAG* plants in various genetic backgrounds grown under LDs at 50 DAS. α -Tubulin was used as a loading control. The numbers below each lane indicate the relative levels of RFT1-FLAG in various genetic backgrounds, calculated by first normalizing each signal against the signal for α -tubulin and then against the value of *gRFT1-FLAG* (first lane).

(D) Quantitative real-time PCR analysis of *OsMADS14* and *OsMADS15* expression in SAMs of *gRFT1-FLAG* plants in various genetic backgrounds grown under LDs at 60 DAS. Results were normalized against the expression levels of *Ubiquitin* based on three biological replicates. The maximum expression level is set to 100%. Asterisks indicate significant differences in gene expression levels between *gRFT1-FLAG Osftip1-1* and *gRFT1-FLAG* (Student's t test, $P < 0.05$). Error bars indicate sd.

(E) Analysis of RFT1-FLAG distribution in CC-SE complexes in leaves of *gRFT1-FLAG* and *gRFT1-FLAG Osftip1-1* plants grown under LDs at 50 DAS by immunogold electron microscopy using anti-FLAG antibody. The upper left panels demonstrate the representative CC-SE complexes. Higher magnification views of CCs or SEs are shown in the upper middle or right panels, respectively. Arrowheads indicate the locations of gold particles. Quantification of RFT1-FLAG immunogold signals in CCs and SEs of *gRFT1-FLAG* (wild-type background) or *gRFT1-FLAG Osftip1-1* (*Osftip1-1* background) is shown in the lower left panel. Over 140 CC-SE complexes on 70 sections from seven different plants of each genotype were analyzed. The data are presented as the mean number of gold particles per μm^2 plus or minus sd. Statistical analysis was performed using a two-tailed unpaired Student's t test. The results are considered statistically significant at $P < 0.05$. The lower right panel shows the frequency histogram of appearance of RFT1-FLAG immunogold signals in companion cells and sieve elements in all examined sections of *gRFT1-FLAG* or *gRFT1-FLAG Osftip1-1*. Asterisks indicate that the frequency we observed companion cells without gold particles is 0 in all sections examined. CC, companion cell; SE, sieve element. Bars = 2 μm in upper left panels and 0.5 μm in upper middle and right panels.

from the start codon included in the gene complementation test (Figures 6B and 6C) was fused to the *GUS* reporter gene. Among 10 independent *ProOsUbDK γ 4:GUS* lines generated, most lines consistently displayed similar *GUS* staining patterns in vascular tissues of various plant organs, such as leaves, leaf sheaths, and roots (Figure 5D; Supplemental Figure 9C). *ProOsUbDK γ 4:GUS* expression was specifically detectable in

the phloem, including companion cells (Figure 5E), a pattern similar to that exhibited by *ProOsFTIP1:GUS* (Figure 2B). Furthermore, transient expression of *Pro35S:OsUbDK γ 4-GFP* in *N. benthamiana* leaf epidermal cells also revealed substantial colocalization of OsUbDK γ 4-GFP with ER-RFP in tobacco cells except for the nuclear localization of OsUbDK γ 4-GFP (Figure 5F). These observations on overlapping tissue expression and

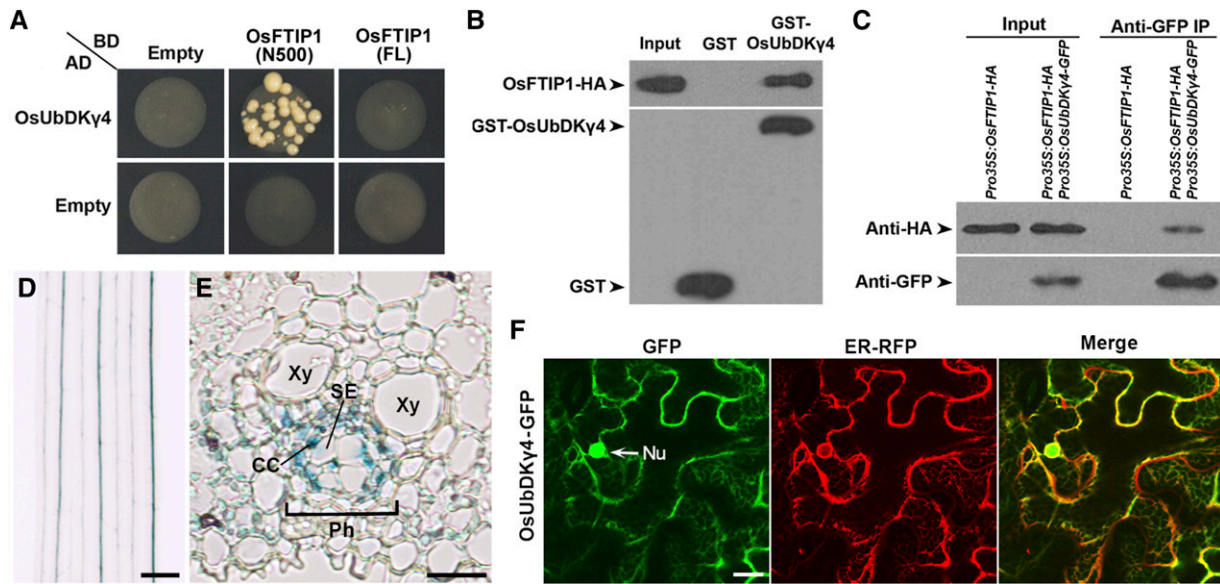


Figure 5. OsFTIP1 Interacts with OsUbDK γ 4.

(A) Yeast two-hybrid assay of interaction between OsUbDK γ 4 and the full-length OsFTIP1 (FL) and its N terminus (amino acids 1–500; N500). Transformed yeast cells were grown on SD-His/-Trp/-Leu medium supplemented with 2 mM 3-amino-1,2,4-triazole. Empty refers to AD- or BD-containing vector only. (B) In vitro GST pull-down assay evaluating interaction between OsUbDK γ 4 and OsFTIP1. HA-tagged OsFTIP1 protein generated from rice protoplasts was incubated with immobilized GST or GST-OsUbDK γ 4, respectively. Immunoblot analysis was performed using either anti-HA (upper panel) or anti-GST (lower panel) antibody. Input, 5% of the protein generated from rice protoplasts. (C) In vivo interaction between OsUbDK γ 4 and OsFTIP1 shown by coimmunoprecipitation. *Pro35S:OsUbDK γ 4-GFP* and *Pro35S:OsFTIP1-HA* were cotransferred to rice protoplasts, and total protein extracts were immunoprecipitated by anti-GFP beads. The input and coimmunoprecipitated protein were detected by either anti-HA (upper panel) or anti-GFP (lower panel) antibody. (D) and (E) GUS staining of a representative *ProOsUbDK γ 4:GUS* line shows *OsUbDK γ 4* expression in a leaf (D) and a transverse section of a leaf (E). CC, companion cell; Ph, phloem; SE, sieve element; Xy, xylem. Bars = 100 μ m in (D) and 10 μ m in (E). (F) Subcellular localization of OsUbDK γ 4-GFP in *N. benthamiana* leaf epidermal cells. OsUbDK γ 4-GFP is mostly colocalized with an ER marker. GFP, GFP fluorescence; ER-RFP, RFP fluorescence of an ER marker; Merge, merge of GFP and RFP; Nu, nucleus. Bar = 10 μ m.

subcellular localization of OsFTIP1 and OsUbDK γ 4, together with their physical interaction at the protein level, strongly imply that OsUbDK γ 4 could be relevant to OsFTIP1 function in the phloem.

OsUbDK γ 4 Affects Flowering Time in Rice under LDs

To investigate whether OsUbDK γ 4 affects rice flowering, we generated *Osubdk γ 4* mutants through CRISPR/Cas9-mediated target mutagenesis. We designed the sgRNA targeted to the region 3' to the translational start site of *OsUbDK γ 4* (Figure 6A) and created two homozygous mutants, *Osubdk γ 4-1* and *Osubdk γ 4-2*, in the absence of the CRISPR/Cas9 transgene. These two mutants contained a 1-bp guanine (G) insertion and a 1-bp thymine (T) deletion (Figure 6A), which resulted in premature termination of OsUbDK γ 4 with only 79 and 82 amino acids, respectively. Examination of the three most likely off-target sites of *OsUbDK γ 4* in *Osubdk γ 4-1* and *Osubdk γ 4-2* did not reveal any unexpected mutations in the putative off-target loci (Supplemental Table 1).

Both *Osubdk γ 4-1* and *Osubdk γ 4-2* exhibited earlier flowering than wild-type plants under LDs (Figures 6B and 6C), indicating that OsUbDK γ 4 delays flowering in rice. To substantiate that the

early-flowering phenotype of *Osubdk γ 4-1* is due to an impaired function of *OsUbDK γ 4*, we transformed homozygous *Osubdk γ 4-1* plants with a genomic construct (*gOsUbDK γ 4*) harboring a 5.5-kb *OsUbDK γ 4* genomic fragment including the 3.1-kb 5' upstream sequence and the 2.4-kb coding sequence plus one intron, and selected seven independent transformants probably containing the single-copy transgene based on a 3:1 Mendelian segregation ratio. All their homozygous progenies at the T2 generation showed similar flowering time to wild-type plants under LDs (Figure 6C), confirming that *OsUbDK γ 4* contributes to repression of flowering in rice under LDs. In addition, we also created 21 independent *Pro35S:OsUbDK γ 4* transgenic lines, among which 18 lines showed different levels of late flowering under LDs. We measured *OsUbDK γ 4* expression in five selected late-flowering lines and found that the degrees of late flowering under LDs in these lines were closely related to the levels of upregulation of *OsUbDK γ 4* expression (Figure 6D), indicating that *OsUbDK γ 4* might have a dosage-dependent effect on suppressing flowering.

We next examined the biological significance of the interaction of OsUbDK γ 4 and OsFTIP1 through genetic analysis. Because of the opposite effects of OsUbDK γ 4 and OsFTIP1 on rice flowering, *Osubdk γ 4-1* and *Osftip1-1* showed completely

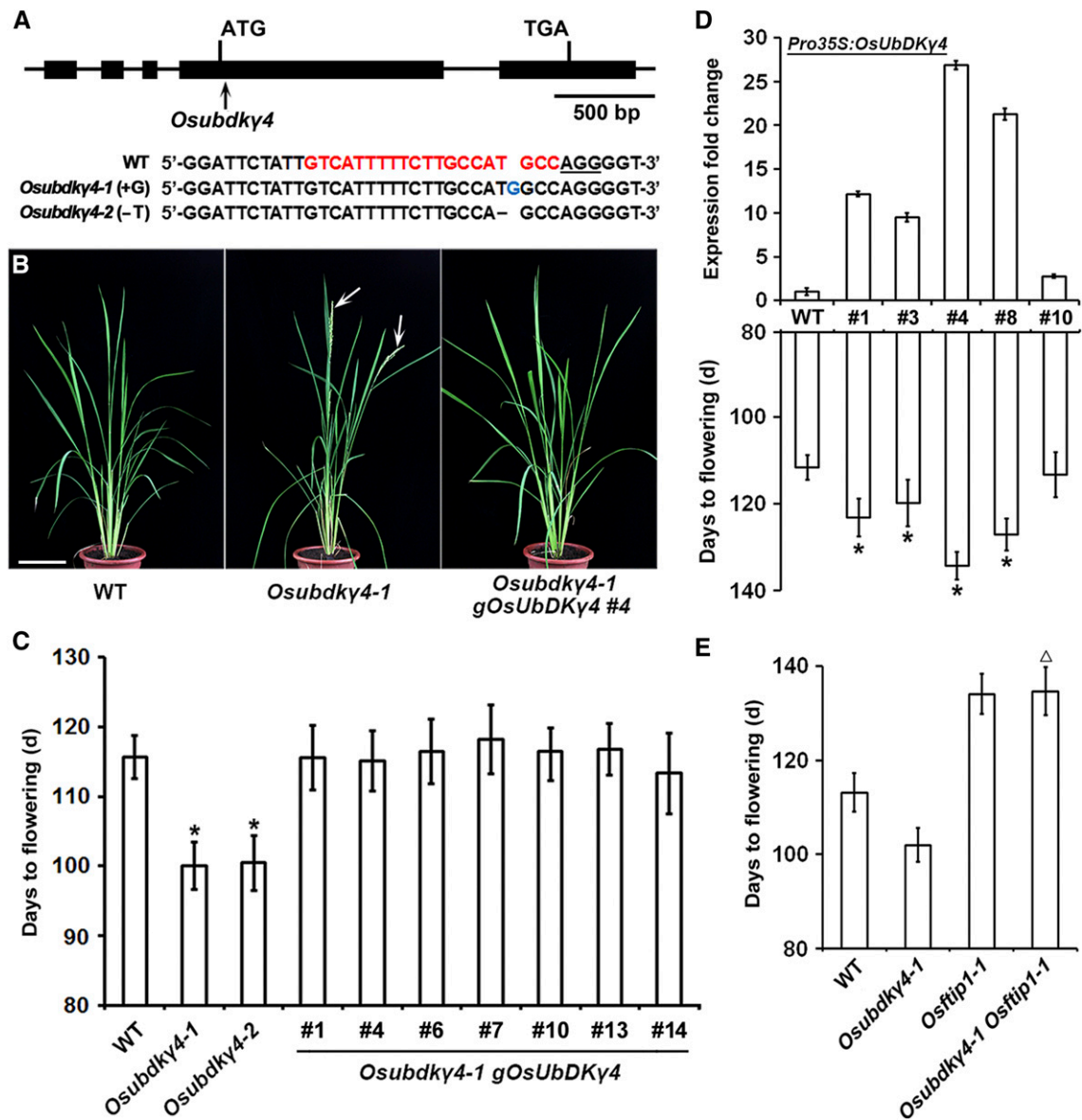


Figure 6. *OsUbDKγ4* Delays Flowering in Rice.

(A) CRISPR/Cas9-mediated target mutagenesis of *OsUbDKγ4*. The upper panel shows a schematic diagram of the *OsUbDKγ4* gene bearing the CRISPR/Cas9 target site indicated by an arrow. Exons and other genomic regions are represented by black boxes and lines, respectively. The lower panel shows alignment of wild-type, *OsSubdkγ4-1*, and *OsSubdkγ4-2* sequences containing the CRISPR/Cas9 target site. A 20-bp CRISPR/Cas9 target sequence adjacent to the underlined protospacer adjacent motif is indicated in red in the wild-type sequence. The newly created *OsSubdkγ4-1* and *OsSubdkγ4-2* mutants contain a 1-bp insertion (G, blue font) and a 1-bp deletion (T, dash), respectively.

(B) *OsSubdkγ4-1* displays earlier flowering than a wild-type plant and a representative *OsSubdkγ4-1* line harboring *gOsUbDKγ4* (#4) grown under LDs at 105 DAS. Arrows indicate panicles. Bar = 15 cm.

(C) Days to flowering of selected *OsSubdkγ4-1* lines harboring *gOsUbDKγ4* at the T2 generation under LDs. $n = 15$; error bars denote sd. Asterisks indicate significant differences in flowering time of *OsSubdkγ4-1* and *OsSubdkγ4-2* compared with that of wild-type and *OsSubdkγ4-1 gOsUbDKγ4* lines (Student's t test, $P < 0.05$).

(D) Upregulation of *OsUbDKγ4* has a dosage-dependent effect on delaying flowering. The upper panel shows *OsUbDKγ4* expression determined by quantitative real-time PCR in independent T2 *Pro35S:OsUbDKγ4* lines grown under LDs at 50 DAS. The levels of gene expression normalized to *Ubiquitin* expression are shown relative to the level in wild-type plants, which was set to 1. The lower panel shows days to flowering of independent *Pro35S:OsUbDKγ4* lines under LDs. $n = 15$; error bars denote sd. Asterisks indicate significant differences in flowering time of *Pro35S:OsUbDKγ4* lines compared with that of wild-type plants (Student's t test, $P < 0.05$).

(E) Days to flowering of *OsSubdkγ4-1 Osftip1-1* under LDs. $n = 15$; error bars denote sd. Open triangle indicates no statistically significant difference in flowering time of *OsSubdkγ4-1 Osftip1-1* compared with that of *Osftip1-1* (Student's t test, $P > 0.05$).

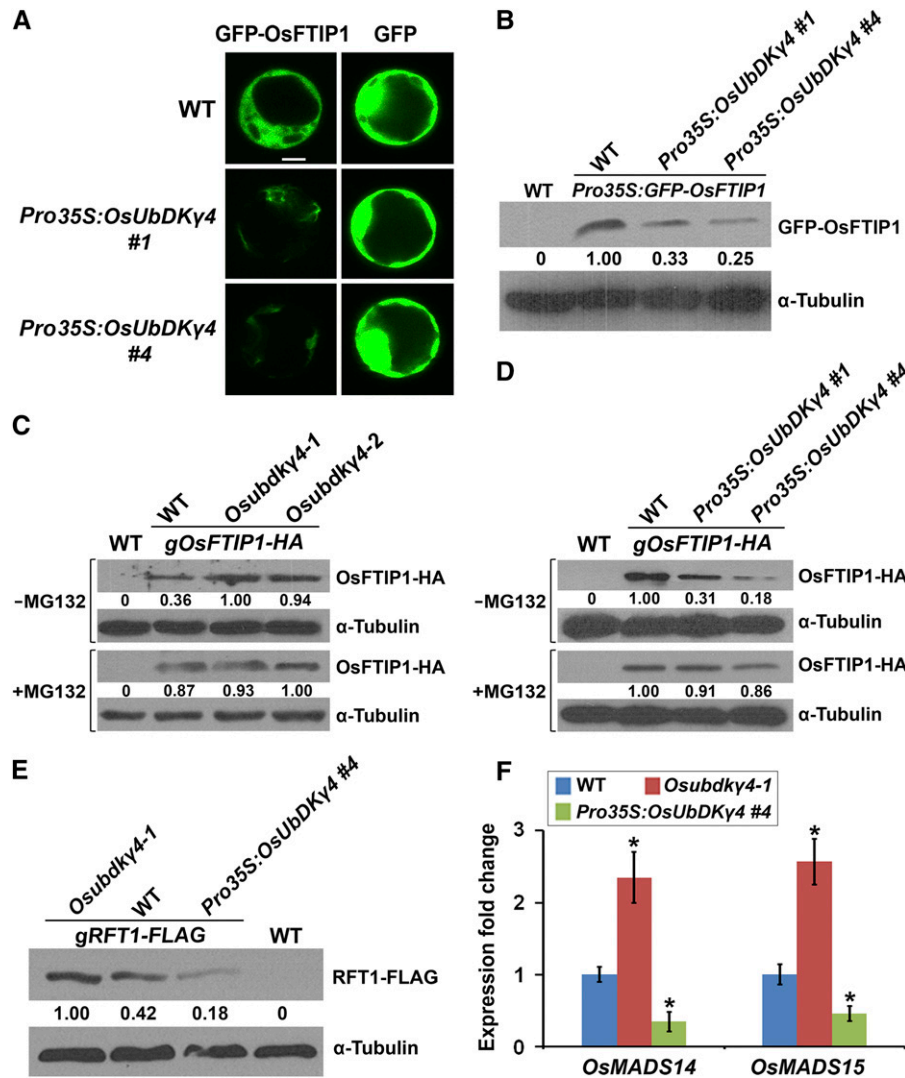


Figure 7. OsUbdK γ 4 Modulates OsFTIP1 Abundance to Affect RFT1 Transport to the SAM.

(A) Detection of GFP fluorescence in mesophyll protoplasts of wild-type and *Pro35S:OsUbdK γ 4* (#1 and #4) plants transformed with *Pro35S:GFP-OsFTIP1* or *Pro35S:GFP*. GFP signals were examined at 16 h after transformation. Bar = 10 μ m.

(B) Immunoblot analysis using anti-GFP antibody shows GFP-OsFTIP1 abundance in mesophyll protoplasts of wild-type and *Pro35S:OsUbdK γ 4* (#1 and #4) plants transformed with *Pro35S:GFP-OsFTIP1*. Protoplast protein was extracted at 16 h after transformation. α -Tubulin was used as a loading control.

(C) and (D) Immunoblot analysis using anti-HA antibody shows OsFTIP1-HA abundance in leaves of *gOsFTIP1-HA* plants in the *OsUbdK γ 4* (C) or *Pro35S:OsUbdK γ 4* background (D) grown under LDs at 50 DAS. Total protein was extracted from leaves mock treated (0.01% Silwet-L77 and 0.2% DMSO) without MG132 or treated with 100 μ M MG132 (plus 0.01% Silwet-L77 and 0.2% DMSO) for 4 h. α -Tubulin was used as a loading control.

(E) Immunoblot analysis using anti-FLAG antibody shows RFT1-FLAG abundance in SAMs of *gRFT1-FLAG* plants in the *OsUbdK γ 4-1* or *Pro35S:OsUbdK γ 4* (#4) background grown under LDs at 50 DAS. α -Tubulin was used as a loading control.

(F) Quantitative real-time PCR analysis of *OsMADS14* and *OsMADS15* expression in SAMs of *OsUbdK γ 4-1* and *Pro35S:OsUbdK γ 4* (#4) grown at 80 DAS under LDs. Results were normalized against the expression levels of *Ubiquitin* based on three biological replicates. The expression levels in wild-type plants are set to 1. Asterisks indicate significant differences in gene expression levels in *OsUbdK γ 4-1* and *Pro35S:OsUbdK γ 4* (#4) compared with those of wild-type plants (Student's *t* test, $P < 0.05$). Error bars indicate sd.

In (B) to (E), the numbers below each lane indicate the relative levels of the protein examined in various genetic backgrounds, calculated by first normalizing each signal against the signal for α -tubulin and then against the highest value in each blot set to 1.

different flowering phenotypes under LDs (Figures 1D, 1E, 6B, and 6C). However, *OsUbdK γ 4-1* *Osftip1-1* double mutants exhibited late flowering similar to *Osftip1-1* (Figure 6E), demonstrating that *OsFTIP1* is genetically epistatic to *OsUbdK γ 4*.

This result, together with the observations on the interaction between OsUbdK γ 4 and OsFTIP1 (Figure 5), suggests that OsUbdK γ 4 exerts its function in controlling flowering time via OsFTIP1.

OsUbDK γ 4 Promotes Degradation of OsFTIP1

Previous studies have suggested that the UBL domain facilitates UBL proteins to interact with the components of the 26S proteasome and promote the targeting of proteolytic substrates to the proteasome (Schauber et al., 1998; Sakata et al., 2003; Ishii et al., 2006). In Arabidopsis, the UBL-domain-containing UbDK γ 4 interacts with Regulatory Particle Non-ATPase 10 (RPN10) and Ubiquitin Fusion Degradation 1, both of which bind to some forms of ubiquitin and mediate substrate delivery to the 26S proteasome (Galvão et al., 2008).

To investigate whether OsUbDK γ 4 could play a similar role to UbDK γ 4 in mediating protein degradation, we first tested the interaction between OsUbDK γ 4 and OsRPN10 in rice. A GST pull-down assay showed that OsRPN10-HA generated from rice protoplasts bound to in vitro-translated GST-OsUbDK γ 4 rather than GST (Supplemental Figure 10A). We also cotransformed *Pro35S:OsUbDK γ 4-GFP* and *Pro35S:OsRPN10-HA* into rice protoplasts and performed coimmunoprecipitation analysis of protein extracts from these protoplasts. The interaction between OsUbDK γ 4-GFP and OsRPN10-HA was only found in protein extracts from the protoplasts transformed with both *Pro35S:OsUbDK γ 4-GFP* and *Pro35S:OsRPN10-HA* (Supplemental Figure 10B). These results demonstrate that OsUbDK γ 4 interacts with OsRPN10, implying that OsUbDK γ 4 may similarly affect substrate delivery to the 26S proteasome.

The interaction of OsUbDK γ 4 with OsFTIP1 and OsRPN10 prompted us to test whether OsUbDK γ 4 could mediate the

degradation of OsFTIP1 through the 26S proteasome. To this end, we transiently expressed *Pro35S:GFP-OsFTIP1* or *Pro35S:GFP* in mesophyll protoplasts of wild-type and *Pro35S:OsUbDK γ 4* transgenic plants (#1 and #4) (Figure 6D). The GFP-OsFTIP1 fluorescence signal was dramatically decreased in *Pro35S:OsUbDK γ 4* protoplasts compared with wild-type protoplasts, whereas the free GFP signal remained unchanged in both *Pro35S:OsUbDK γ 4* and wild-type protoplasts (Figure 7A). Immunoblot analysis confirmed that GFP-OsFTIP1 abundance was reduced in *Pro35S:OsUbDK γ 4* mesophyll protoplasts compared with wild-type ones (Figure 7B; Supplemental Figure 12B), indicating that OsUbDK γ 4 activity is inversely correlated with OsFTIP1 protein abundance in rice mesophyll protoplasts.

To further examine the in vivo effect of OsUbDK γ 4 on OsFTIP1 abundance in rice, we crossed *gOsFTIP1-HA* (#5) (Supplemental Figures 3B and 3C) with *Osubdk γ 4* mutants and *Pro35S:OsUbDK γ 4* (#1 and #4) transgenic plants (Figures 6C and 6D) and measured OsFTIP1-HA protein levels in leaves of the resulting homozygous progenies grown under LDs at 50 DAS treated with or without MG132, a 26S proteasome inhibitor. In the absence of MG132 treatment, OsFTIP1 levels were increased in *Osubdk γ 4*, but decreased in *Pro35S:OsUbDK γ 4*, whereas under MG132 treatment, OsFTIP1 levels remained almost unaltered in both *Osubdk γ 4* and *Pro35S:OsUbDK γ 4* plants (Figures 7C and 7D; Supplemental Figures 12C and 12D). These results, together with the observation that OsUbDK γ 4 interacts with OsFTIP1, indicate that OsUbDK γ 4 recruits OsFTIP1 for degradation by the 26S

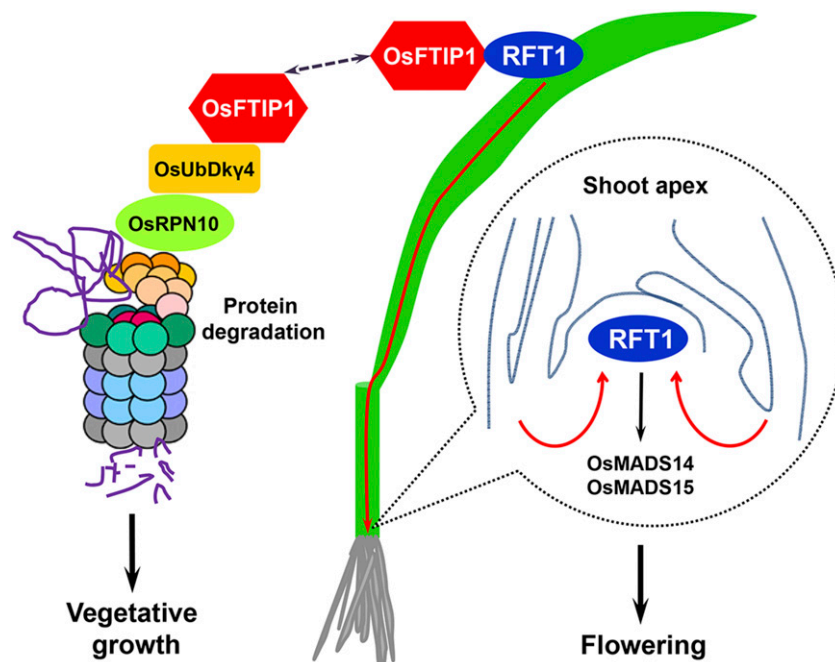


Figure 8. OsFTIP1-Mediated Regulation of RFT1 Transport Is Negatively Regulated by OsUbDK γ 4 in Rice.

OsFTIP1 is required for RFT1 export from companion cells to sieve elements in rice leaves under LDs and affects RFT1 transport to the SAM for further regulating other genes involved in floral meristem development, such as *OsMADS14* and *OsMADS15*. OsUbDK γ 4 interacts with OsFTIP1 and mediates OsFTIP1 degradation in leaves. This contributes to modulation of RFT1 trafficking from leaves to the SAM, thus regulating flowering time in rice under LDs. Red arrows indicate RFT1 transport, while black arrows indicate various promotive effects. Dotted arrow indicates the regulation of OsFTIP1 abundance.

proteasome in rice leaves. In contrast, *OsFTIP1* mRNA levels were not changed in either *Osubdkγ4* or *Pro35S:OsUbdKγ4* plants (Supplemental Figure 10C), implying that OsUbdKγ4 is unlikely to transcriptionally affect *OsFTIP1* expression.

Since *OsFTIP1* affects RFT1 transport from leaves to the SAM (Figure 4), we then tested whether the effect of OsUbdKγ4 on *OsFTIP1* abundance in leaves eventually influences RFT1 levels in the SAM. We crossed *gRFT1-FLAG* (#2) (Supplemental Figures 7A and 7B) with *Osubdkγ4-1* and *Pro35S:OsUbdKγ4* (#4) and measured RFT1-FLAG protein levels in the SAMs of the resulting homozygous progenies grown at 50 DAS under LDs. In agreement with the changes in *OsFTIP1* levels in leaves (Figures 7C and 7D), RFT1-FLAG abundance was increased in *Osubdkγ4-1*, but decreased in *Pro35S:OsUbdKγ4* (#4) (Figure 7E; Supplemental Figure 12E). Consistently, the expression of *OsMADS14* and *OsMADS15* was also upregulated in *Osubdkγ4-1* but downregulated in *Pro35S:OsUbdKγ4* (#4) (Figure 7F). Meanwhile, yeast two-hybrid and in vitro pull-down assays revealed that OsUbdKγ4 did not interact with RFT1 (Supplemental Figure 11). Thus, these observations suggest that OsUbdKγ4 mediates the degradation of *OsFTIP1*, which affects RFT1 transport to the SAM. This in turn regulates the expression of *OsMADS14* and *OsMADS15* under LDs.

DISCUSSION

Over the centuries, domestication and breeding of rice, one of the most important cereal crops in the world, have significantly expanded the geographical regions in which rice varieties are grown. As a critical agronomic trait that determines crop yield and regional adaptability, flowering time in rice is controlled by a complex network of regulatory pathways that responds to various environmental signals, which typically include different photoperiods in a broad range of latitudes (Izawa, 2007; Song et al., 2015). In particular, adaptation of rice varieties to the cold regions of northern high-latitudes permits rice to flower in response to typical LD conditions to ensure timely grain production before the onset of the cold season (Izawa, 2007). Although two rice orthologs of *Arabidopsis* FT, *Hd3a* and *RFT1*, have been identified as specific florigen required for rice flowering under SD and LD conditions, respectively (Tamaki et al., 2007; Komiya et al., 2008, 2009), how they make their voyage from leaves to the SAM in response to photoperiods remains elusive. Here, we have shown that *OsFTIP1*, a rice ortholog of *Arabidopsis* FTIP1 (Liu et al., 2012), specifically regulates rice flowering time under LDs through modulating RFT1 transport from companion cells to sieve elements. In addition, we revealed that a UBL protein, OsUbdKγ4, interacts with *OsFTIP1* and controls *OsFTIP1* abundance in rice leaves through the 26S proteasome, thus mediating RFT1 transport to the SAM and the resulting flowering time under LDs (Figure 8). These findings shed light on the hitherto unknown mechanisms underlying the regulation of florigen transport in the monocot crop rice and suggest that dynamic modulation of FTIP1-like MCTP levels in leaves is integral to their effects on florigen transport in source tissues.

Compared with the advanced understanding of flowering regulatory networks in *Arabidopsis*, flowering time research in monocots has been partially impeded by inefficient and relatively

time-consuming reverse genetics approaches for creating or screening inheritable genetic materials of interest. While the regulators of rice flowering pathways were identified by mapping quantitative trait loci (Yano et al., 2000; Rensink and Buell, 2004), reverse genetics approaches including RNAi have recently been intensively used to generate knockout or knockdown lines for functional studies of flowering regulators in rice. For example, characterization of the rice florigen genes *Hd3a* and *RFT1* was based on RNAi lines created in the *japonica* cultivar Norin 8 (Komiya et al., 2009). However, further application of the resulting RNAi lines for elucidating the regulatory mechanisms involving florigen is difficult because of the inherent disadvantages of RNAi lines, including the presence of early inserted transgenes, incomplete knockdown efficiency, or possible off-target effects. In this study, we systematically performed CRISPR/Cas9-mediated target mutagenesis of genes involved in florigen transport, including *OsUbdKγ4*, *OsFTIP1*, *Hd3a*, and *RFT1*, and created the corresponding rice mutants without the CRISPR/Cas9 transgenes in the *japonica* cultivar Nipponbare. These mutants, which have no detectable off-target mutations (Supplemental Table 1), exhibit stable and inheritable flowering phenotypes, thus serving as essential genetic materials for further elucidation of the molecular mechanisms underlying florigen transport in rice.

Our investigation of these mutants and other derived rice plants has provided several pieces of evidence that support an essential role of *OsFTIP1* in mediating RFT1 transport and its regulation of rice flowering specifically under LDs. First, both *OsFTIP1* and RFT1 promote rice flowering mainly under LDs, as impairing their activity in genome-edited *Osttip1* and *rft1* mutants delays flowering only under LDs. Second, *OsFTIP1* and RFT1 share similar mRNA expression patterns in the phloem and protein subcellular localization in plant cells. More importantly, they interact with each other in vitro and also in vivo in rice leaves. Third, the effect of RFT1-FLAG on promoting flowering under LDs is compromised in *Osttip1* mutants. This is due to the decreased abundance of RFT1-FLAG in the SAM, although RFT1-FLAG abundance in leaves is not altered, indicating that RFT1 transport from leaves to the SAM is impaired in *Osttip1* mutants. Fourth, *OsFTIP1* is only found in phloem companion cells. In *Osttip1* mutants, RFT1-FLAG accumulates to high levels in companion cells, but decreases in sieve elements, suggesting that *OsFTIP1* promotes RFT1-FLAG export from companion cells to sieve elements in the phloem. Taken together, these findings reveal that *OsFTIP1* plays an indispensable role in contributing to the transport of a LD-specific florigen, RFT1, from the leaves to the SAM in rice.

Since FT-like florigen have been identified in various flowering species and have been proposed to be universal and functionally exchangeable signals (Zeevaart, 1976, 2006; Putterill and Varkonyi-Gasic, 2016), research on the conservation and diversification of flowering mechanisms in flowering plants has been intensively focused on characterizing these florigen proteins and their regulatory components under various environmental conditions. A comparison of photoperiodic control of flowering in *Arabidopsis* and rice revealed that dicots and monocots may have evolved independent upstream regulatory pathways to control the expression of florigen genes under various photoperiods, in which evolutionarily conserved regulators are only present to a limited extent (Komiya et al., 2009; Shrestha et al., 2014). In particular, the major flowering pathways that regulate florigen gene expression in

Arabidopsis and rice under LDs are mostly different. Transcription of the florigen gene *FT* in Arabidopsis is activated by the nuclear zinc-finger transcriptional regulator CO in response to LDs (Samach et al., 2000; Suárez-López et al., 2001; An et al., 2004), whereas a unique B-type response regulator, Early heading date 1, mainly contributes to activation of the LD-specific florigen gene *RFT1* in rice under LDs (Doi et al., 2004). Despite this major difference in regulating florigen gene expression in rice and Arabidopsis, our findings suggest that florigen transport from companion cells to sieve elements under LDs could be mediated by similar members in the family of MCTPs, including rice OsFTIP1 and its Arabidopsis ortholog FTIP1 (Liu et al., 2012), both of which are membrane-anchored multiple C2 domain proteins and present in phloem companion cells, but not in sieve elements. It would be interesting to further clarify the function of other FTIP1-like MCTPs to explore whether the conservation of the florigen transport mechanism is also applicable to rice flowering behavior under SDs, which is mainly regulated through another SD-specific florigen gene *Hd3a* (Tamaki et al., 2007; Komiya et al., 2008). In addition, as both *OsFTIP1* and *FTIP1* are expressed in vascular tissues of various plant organs, including reproductive organs and roots, in rice and Arabidopsis (Liu et al., 2012), respectively, they may play multiple roles in plant development. Generating combinatorial multiple mutants among MCTPs may help to address whether these proteins play redundant roles in regulating various developmental processes.

It is noteworthy that OsFTIP1 abundance in rice leaves is modulated by a UBL-domain-containing protein OsUbdK γ 4. Like some other UBL proteins, OsUbdK γ 4 interacts with the components of the 26S proteasome, such as OsRPN10, which mediates delivery of proteolytic substrates to the proteasome (Schauber et al., 1998; Sakata et al., 2003; Ishii et al., 2006; Galvão et al., 2008). Both OsUbdK γ 4 and OsFTIP1 are associated with ER in tobacco cells, implying that they could potentially be components of the ER-derived 26S proteasome substrates. Consistently, inhibition of 26S proteasome activity by MG132 abolishes the effect of OsUbdK γ 4 on modulating OsFTIP1 abundance in rice leaves. Thus, the interaction between OsFTIP1 and OsUbdK γ 4 as well as their overlapping tissue expression patterns and sub-cellular localizations suggests that OsUbdK γ 4 tightly controls OsFTIP1 levels in the phloem by mediating OsFTIP1 degradation through the 26S proteasome (Figure 8). This explains why *OsFTIP1* is genetically epistatic to *OsUbdK γ 4* in affecting rice flowering time under LDs. As a result, OsUbdK γ 4 indirectly affects RFT1 transport to the SAM under LDs, although OsUbdK γ 4 itself does not interact with RFT1. These findings suggest that the proteasomal degradation pathway is ultimately important for regulating florigen transport in rice under LDs. Further investigation of the temporal and spatial regulation of this pathway in various flowering plants will advance our understanding of the orchestrated signal transduction networks required for florigen production and transport in response to environmental signals.

METHODS

Plant Materials and Growth Conditions

Rice (*Oryza sativa* ssp *japonica* cultivar Nipponbare) was grown in climate chambers under SDs (10 h light at 30°C/14 h dark at 25°C) or LDs (14 h light

at 30°C/10 h dark at 25°C) with a relative humidity of ~70%. Light (500–700 nm, 100–200 $\mu\text{mol m}^{-2} \text{s}^{-1}$) was provided by fluorescent white light tubes. Flowering time was measured as the number of days from germination to the heading stage.

Plasmid Construction and Plant Transformation

To construct *pCAMBIA1300-CAS9-Os-OsFTIP1/RFT1/Hd3a/OsUbdK γ 4*, the psgR-CAS9-Os backbone was digested by *Bbs*I and ligated with the synthesized sgRNA oligos. The resulting fragments were subcloned into the *Hind*III/*Eco*RI site of the pCAMBIA1300 binary vector for stable rice transformation (Feng et al., 2014). To create RNAi constructs, the gene-specific region of *OsFTIP1* was selected and amplified. The PCR product was cloned into pZH2bik as previously described (Kuroda et al., 2010). To construct *Pro35S:OsUbdK γ 4*, the *OsUbdK γ 4* cDNA sequence was amplified and cloned into Pro35S-pENTR. To construct *gOsFTIP1-HA*, *gRFT1-FLAG*, and *ProRFT1:FLAG*, the corresponding genomic fragments were amplified and cloned into pENTR-6HA, pENTR-3FLAG and pENTR-6FLAG, respectively. Transfer of the DNA fragment from the entry clone to pHGW by LR reaction was performed according to the manufacturer's instructions (Invitrogen). The primers for creating the above constructs are listed in Supplemental Table 3. Transgenic rice plants were generated by *Agrobacterium tumefaciens*-mediated transformation of rice calli as previously described (Toki et al., 2006). All rice transgenic plants were selected on 50 $\mu\text{g/mL}$ hygromycin.

Expression Analysis

Total RNA was isolated with an RNeasy Plant Mini Kit (Qiagen) and reverse-transcribed with the ThermoScript RT-PCR system (Invitrogen) according to the manufacturer's instructions. Quantitative real-time PCR was performed in triplicates on a CFX38 real-time system (Bio-Rad) with iQ SYBR Green Supermix (Bio-Rad). The relative expression levels were calculated as previously reported (Liu et al., 2007). Expression analysis was performed with three biological replicates. All primers used for gene expression analysis are listed in Supplemental Table 3.

Histochemical Analysis of GUS Expression

Tissues for GUS staining were first infiltrated with staining solution (50 mM sodium phosphate buffer, pH 7.0, 0.5 mM potassium ferrocyanide, 0.5 mM potassium ferricyanide, and 0.5 mg/mL X-Gluc) in a vacuum chamber and subsequently incubated with the same solution at 37°C for 6 h. Samples were dehydrated through an ethanol series and an ethanol/histoclear series and finally embedded in paraffin for sectioning at a thickness of 10 μm using an Ultracut UCT ultramicrotome (Leica).

Transient Expression of Proteins in Tobacco Cells and Rice Protoplasts

The coding sequences of *OsFTIP1* and *OsUbdK γ 4* were amplified and cloned into pGreen-GFP, while the coding sequence of *RFT1* was amplified and cloned into pGreen-RFP. *Agrobacterium* cultures grown overnight with these expression vectors were harvested and resuspended with infiltration buffer (10 mM MES, pH 5.6, 10 mM MgCl₂, and 100 μM aceto-syringone) to an OD₆₀₀ of 0.5. To compare protein localization, equal volumes of infiltration solutions containing different expression vectors were mixed together and then infiltrated into the abaxial surface of leaves of 3-week-old tobacco (*Nicotiana benthamiana*) plants with syringes. The leaves were examined 40 to 48 h after infiltration under a confocal microscope. Isolation of rice protoplast and PEG-mediated transfection were performed as previously described (Bart et al., 2006). After transformation, the protoplasts were incubated in darkness for 12 to 16 h before being

examined under a confocal microscope or collected for immunoblot analysis.

Yeast Two-Hybrid Assay

The coding sequences of *OsFTIP1*, *RFT1*, *Hd3a*, and *OsUbdK γ 4* were amplified and cloned into pGBKT7 and pGADT7 (Clontech), respectively. Yeast two-hybrid assays were performed using the Yeastmaker Yeast Transformation System 2 according to the manufacturer's instructions (Clontech).

GST Pull-Down Assay

To produce GST-tagged proteins, the cDNAs encoding RFT1, Hd3a, and OsUbdK γ 4 were cloned into pGEX-6p-2 vector (Pharmacia), respectively. These constructs and the empty pGEX-6p-2 vector were transformed into *Escherichia coli* Rosetta (DE3) (Novagen), and protein expression was induced by isopropyl- β -D-thiogalactoside at 16°C. The soluble GST fusion proteins were extracted and immobilized on MagneGST Glutathione Particles (Promega) for subsequent pull-down assays. To produce HA-tagged OsFTIP1, OsRPN10, and RFT1 proteins, the cDNAs encoding these proteins were cloned into pGreen-HA vector. The resulting plasmids were transformed into rice protoplasts to generate OsFTIP1-HA, OsRPN10-HA, or RFT1-HA protein, respectively. The HA-tagged proteins were then incubated with the immobilized GST and GST fusion proteins. Proteins retained on the beads were resolved by SDS-PAGE and detected with anti-HA antibody (sc-7392; Santa Cruz Biotechnology; 1:1000 dilution).

Coimmunoprecipitation Experiment

Total proteins were isolated from transgenic rice plants or transformed protoplasts with a Plant Total Protein Extraction Kit (Sigma-Aldrich). The protein extracts were then incubated with magnetic beads (Life Technologies) and anti-FLAG (F3165; Sigma-Aldrich; 1:1000 dilution) or anti-GFP antibody (sc-9996; Santa Cruz Biotechnology; 1:1000 dilution) at 4°C for 2 h. The total protein extracts as inputs and the immunoprecipitated proteins bound by beads were resolved by SDS-PAGE and detected by anti-HA antibody (sc-7392; Santa Cruz Biotechnology; 1:1000 dilution).

BiFC Analysis

The cDNAs encoding OsFTIP1 and RFT1 were cloned into primary pSAT1 vectors. The resulting cassettes including fusion proteins and the constitutive promoters were cloned into a pGreen binary vector pHY105 and transformed into *Agrobacterium* for BiFC analysis as previously published (Sparkes et al., 2006).

Immunoblotting

To isolate rice SAMs, we removed all leaves surrounding the SAMs and collected SAMs of around 400 μ m in height and 500 μ m in diameter under the microscope. For total protein extraction, rice tissues were ground in liquid nitrogen and resuspended in Pierce IP buffer (25 mM Tris-HCl, pH 7.4, 150 mM NaCl, 1% Nonidet P-40, 1 mM EDTA, and 5% glycerol) with freshly added 1 mM PMSF and 1 \times protease inhibitor cocktail (Roche). Protein concentrations were determined by the Bio-Rad protein assay. Total protein (25–30 μ g) of each sample was resolved by SDS-polyacrylamide gel electrophoresis and detected with various antibodies. Immunoblots were developed using SuperSignal West Pico or West Femto Chemiluminescent Substrate (Thermo Scientific). Densitometric analysis of immunoblot results was performed using ImageJ software (National Institutes of Health).

Immunogold Transmission Electron Microscopy

Immunoelectron microscopy was performed as previously described (Liu et al., 2012). Samples were fixed in paraformaldehyde-glutaraldehyde solution (2 and 2.5%, respectively) overnight at room temperature and imbedded in LR white medium (EMS). Ultrathin sections mounted on nickel grids were blocked with 1% BSA in TTBS (20 mM Tris, 500 mM NaCl, and 0.05% Tween 20, pH 7.5) for 30 min and then incubated with anti-HA or anti-FLAG antibody at 1:5 (v/v) for 1 h. After washing with TTBS thrice, grids were incubated for 40 min with 15-nm gold-conjugated goat anti-mouse antibody (EMS) that was diluted 1:20 with blocking solution. The grids were subsequently washed with TTBS and distilled water. After tissue staining with 2% uranyl acetate for 15 min at room temperature, photomicrographs were taken using a transmission electron microscope (Jeol JEM-1230). For quantitatively analyzing immunogold labeling, electron micrographs of randomly photographed immunogold-labeled transverse sections were digitized. The number of gold particles and the cell area were measured by ImageJ. We analyzed 70 individual sections from seven different plants of each genotype for calculating the density of gold particles throughout the projected cell area. The results were presented as the mean number of gold particles per μ m² plus or minus the SD and statistically evaluated by a two-tailed paired Student's *t* test.

Accession Numbers

Sequence data from this article can be found in the GenBank/EMBL data libraries under the following accession numbers: *OsFTIP1* (Os06g0614000), *OsUbdK γ 4* (Os02g0290500), *Hd3a* (Os06g0157700), *RFT1* (Os06g0157500), *OsMADS14* (Os03g0752800), *OsMADS15* (Os07g0108900), *OsRPN10* (Os03g0243300), and *Ubiquitin* (Os03g0234200).

Supplemental Data

Supplemental Figure 1. Bioinformatic Analysis of OsFTIP1 Protein Sequence.

Supplemental Figure 2. Downregulation of *OsFTIP1* Delays Flowering in Rice.

Supplemental Figure 3. Complementation of *Osftip1-1* by Two *OsFTIP1* Genomic Fragments.

Supplemental Figure 4. *OsFTIP1* Is Mainly Expressed in Vascular Tissues.

Supplemental Figure 5. Characterization of *hd3a* and *rft1* Mutants.

Supplemental Figure 6. Colocalization of RFT1-RFP and GFP-OsFTIP1 or ER-GFP in *N. benthamiana* Leaf Epidermal Cells.

Supplemental Figure 7. Generation and Characterization of *gRFT1-FLAG* Transgenic Plants.

Supplemental Figure 8. Control Experiments for Measuring OsFTIP1-HA, RFT1-FLAG, and Free FLAG Localization by Immunogold Electron Microscopy.

Supplemental Figure 9. Expression Patterns of *OsUbdK γ 4*.

Supplemental Figure 10. OsUbdK γ 4 Interacts with OsRPN10.

Supplemental Figure 11. OsUbdK γ 4 Does Not Interact with RFT1.

Supplemental Figure 12. Densitometric Analyses of Immunoblots Using Image J.

Supplemental Table 1. Examination of the Sequences on Putative Off-Target Sites.

Supplemental Table 2. List of Potential OsFTIP1 Interacting Proteins Isolated from Yeast Two-Hybrid Screening.

Supplemental Table 3. List of Primers Used in This Study.

ACKNOWLEDGMENTS

We thank Jian-Kang Zhu for providing the psgR-CAS9-Os vector and members of the Yu lab for discussion and comments on the manuscript. This work was supported by the Singapore National Research Foundation Investigatorship Programme (NRF-NRFI2016-02), the National Natural Science Foundation of China (Grant 31529001), and the intramural research support from National University of Singapore and Temasek Life Sciences Laboratory.

AUTHOR CONTRIBUTIONS

S.S., Y.C., and H.Y. conceived and designed the experiments. S.S., Y.C., L.L., Y.W., S.B., X.Z., and Z.W.N.T. performed the experiments. S.S., Y.C., C.M., Y.G. and H.Y. analyzed the data. S.S., Y.C., and H.Y. wrote the manuscript. All authors read and approved of the manuscript.

Received September 19, 2016; revised February 9, 2017; accepted March 1, 2017; published March 2, 2017.

REFERENCES

- An, H., Roussot, C., Suárez-López, P., Corbesier, L., Vincent, C., Piñeiro, M., Hepworth, S., Mouradov, A., Justin, S., Turnbull, C., and Coupland, G. (2004). CONSTANS acts in the phloem to regulate a systemic signal that induces photoperiodic flowering of *Arabidopsis*. *Development* **131**: 3615–3626.
- Balla, A., and Balla, T. (2006). Phosphatidylinositol 4-kinases: old enzymes with emerging functions. *Trends Cell Biol.* **16**: 351–361.
- Bart, R., Chern, M., Park, C.-J., Bartley, L., and Ronald, P.C. (2006). A novel system for gene silencing using siRNAs in rice leaf and stem-derived protoplasts. *Plant Methods* **2**: 13.
- Corbesier, L., Vincent, C., Jang, S., Fornara, F., Fan, Q., Searle, I., Giakountis, A., Farrona, S., Gissot, L., Turnbull, C., and Coupland, G. (2007). FT protein movement contributes to long-distance signaling in floral induction of *Arabidopsis*. *Science* **316**: 1030–1033.
- Doi, K., Izawa, T., Fuse, T., Yamanouchi, U., Kubo, T., Shimatani, Z., Yano, M., and Yoshimura, A. (2004). Ehd1, a B-type response regulator in rice, confers short-day promotion of flowering and controls FT-like gene expression independently of Hd1. *Genes Dev.* **18**: 926–936.
- Feng, Z., et al. (2014). Multigeneration analysis reveals the inheritance, specificity, and patterns of CRISPR/Cas-induced gene modifications in *Arabidopsis*. *Proc. Natl. Acad. Sci. USA* **111**: 4632–4637.
- Fruman, D.A., Meyers, R.E., and Cantley, L.C. (1998). Phosphoinositide kinases. *Annu. Rev. Biochem.* **67**: 481–507.
- Fulton, L., Batoux, M., Vaddepalli, P., Yadav, R.K., Busch, W., Andersen, S.U., Jeong, S., Lohmann, J.U., and Schneitz, K. (2009). DETORQUEO, QUIRKY, and ZERZAUST represent novel components involved in organ development mediated by the receptor-like kinase STRUBBELIG in *Arabidopsis thaliana*. *PLoS Genet.* **5**: e1000355.
- Galvão, R.M., Kota, U., Soderblom, E.J., Goshe, M.B., and Boss, W.F. (2008). Characterization of a new family of protein kinases from *Arabidopsis* containing phosphoinositide 3/4-kinase and ubiquitin-like domains. *Biochem. J.* **409**: 117–127.
- Hagiwara, W.E., Uwatoko, N., Sasaki, A., Matsubara, K., Nagano, H., Onishi, K., and Sano, Y. (2009). Diversification in flowering time due to tandem FT-like gene duplication, generating novel Mendelian factors in wild and cultivated rice. *Mol. Ecol.* **18**: 1537–1549.
- Hayama, R., Yokoi, S., Tamaki, S., Yano, M., and Shimamoto, K. (2003). Adaptation of photoperiodic control pathways produces short-day flowering in rice. *Nature* **422**: 719–722.
- Ishii, T., Funakoshi, M., and Kobayashi, H. (2006). Yeast Pth2 is a UBL domain-binding protein that participates in the ubiquitin-proteasome pathway. *EMBO J.* **25**: 5492–5503.
- Izawa, T. (2007). Adaptation of flowering-time by natural and artificial selection in *Arabidopsis* and rice. *J. Exp. Bot.* **58**: 3091–3097.
- Jaeger, K.E., and Wigge, P.A. (2007). FT protein acts as a long-range signal in *Arabidopsis*. *Curr. Biol.* **17**: 1050–1054.
- Jang, S., Torti, S., and Coupland, G. (2009). Genetic and spatial interactions between FT, TSF and SVP during the early stages of floral induction in *Arabidopsis*. *Plant J.* **60**: 614–625.
- Kardailsky, I., Shukla, V.K., Ahn, J.H., Dagenais, N., Christensen, S.K., Nguyen, J.T., Chory, J., Harrison, M.J., and Weigel, D. (1999). Activation tagging of the floral inducer FT. *Science* **286**: 1962–1965.
- Kobayashi, Y., Kaya, H., Goto, K., Iwabuchi, M., and Araki, T. (1999). A pair of related genes with antagonistic roles in mediating flowering signals. *Science* **286**: 1960–1962.
- Komiya, R., Yokoi, S., and Shimamoto, K. (2009). A gene network for long-day flowering activates RFT1 encoding a mobile flowering signal in rice. *Development* **136**: 3443–3450.
- Komiya, R., Ikegami, A., Tamaki, S., Yokoi, S., and Shimamoto, K. (2008). Hd3a and RFT1 are essential for flowering in rice. *Development* **135**: 767–774.
- Kuroda, M., Kimizu, M., and Mikami, C. (2010). A simple set of plasmids for the production of transgenic plants. *Biosci. Biotechnol. Biochem.* **74**: 2348–2351.
- Liu, C., Zhou, J., Bracha-Drori, K., Yalovsky, S., Ito, T., and Yu, H. (2007). Specification of *Arabidopsis* floral meristem identity by repression of flowering time genes. *Development* **134**: 1901–1910.
- Liu, L., Zhu, Y., Shen, L., and Yu, H. (2013). Emerging insights into florigen transport. *Curr. Opin. Plant Biol.* **16**: 607–613.
- Liu, L., Liu, C., Hou, X., Xi, W., Shen, L., Tao, Z., Wang, Y., and Yu, H. (2012). FTIP1 is an essential regulator required for florigen transport. *PLoS Biol.* **10**: e1001313.
- Mathieu, J., Warthmann, N., Küttner, F., and Schmid, M. (2007). Export of FT protein from phloem companion cells is sufficient for floral induction in *Arabidopsis*. *Curr. Biol.* **17**: 1055–1060.
- Nelson, B.K., Cai, X., and Nebenführ, A. (2007). A multicolored set of in vivo organelle markers for co-localization studies in *Arabidopsis* and other plants. *Plant J.* **51**: 1126–1136.
- Putterill, J., and Varkonyi-Gasic, E. (2016). FT and florigen long-distance flowering control in plants. *Curr. Opin. Plant Biol.* **33**: 77–82.
- Rensink, W.A., and Buell, C.R. (2004). *Arabidopsis* to rice. Applying knowledge from a weed to enhance our understanding of a crop species. *Plant Physiol.* **135**: 622–629.
- Sakata, E., Yamaguchi, Y., Kurimoto, E., Kikuchi, J., Yokoyama, S., Yamada, S., Kawahara, H., Yokosawa, H., Hattori, N., Mizuno, Y., Tanaka, K., and Kato, K. (2003). Parkin binds the Rpn10 subunit of 26S proteasomes through its ubiquitin-like domain. *EMBO Rep.* **4**: 301–306.
- Samach, A., Onouchi, H., Gold, S.E., Ditta, G.S., Schwarz-Sommer, Z., Yanofsky, M.F., and Coupland, G. (2000). Distinct roles of CONSTANS target genes in reproductive development of *Arabidopsis*. *Science* **288**: 1613–1616.
- Schauber, C., Chen, L., Tongaonkar, P., Vega, I., Lambertson, D., Potts, W., and Madura, K. (1998). Rad23 links DNA repair to the ubiquitin/proteasome pathway. *Nature* **391**: 715–718.
- Shrestha, R., Gómez-Ariza, J., Brambilla, V., and Fornara, F. (2014). Molecular control of seasonal flowering in rice, *Arabidopsis* and temperate cereals. *Ann. Bot. (Lond.)* **114**: 1445–1458.

- Song, Y.H., Shim, J.S., Kinmonth-Schultz, H.A., and Imaizumi, T.** (2015). Photoperiodic flowering: time measurement mechanisms in leaves. *Annu. Rev. Plant Biol.* **66**: 441–464.
- Sparkes, I.A., Runions, J., Kearns, A., and Hawes, C.** (2006). Rapid, transient expression of fluorescent fusion proteins in tobacco plants and generation of stably transformed plants. *Nat. Protoc.* **1**: 2019–2025.
- Suárez-López, P., Wheatley, K., Robson, F., Onouchi, H., Valverde, F., and Coupland, G.** (2001). CONSTANS mediates between the circadian clock and the control of flowering in *Arabidopsis*. *Nature* **410**: 1116–1120.
- Tamaki, S., Matsuo, S., Wong, H.L., Yokoi, S., and Shimamoto, K.** (2007). Hd3a protein is a mobile flowering signal in rice. *Science* **316**: 1033–1036.
- Taoka, K., et al.** (2011). 14-3-3 proteins act as intracellular receptors for rice Hd3a florigen. *Nature* **476**: 332–335.
- Tian, H., Baxter, I.R., Lahner, B., Reinders, A., Salt, D.E., and Ward, J.M.** (2010). *Arabidopsis* NPCC6/NaKR1 is a phloem mobile metal binding protein necessary for phloem function and root meristem maintenance. *Plant Cell* **22**: 3963–3979.
- Toki, S., Hara, N., Ono, K., Onodera, H., Tagiri, A., Oka, S., and Tanaka, H.** (2006). Early infection of scutellum tissue with *Agrobacterium* allows high-speed transformation of rice. *Plant J.* **47**: 969–976.
- Vaddepalli, P., Herrmann, A., Fulton, L., Oelschner, M., Hillmer, S., Stratil, T.F., Fastner, A., Hammes, U.Z., Ott, T., Robinson, D.G., and Schneitz, K.** (2014). The C2-domain protein QUIRKY and the receptor-like kinase STRUBBELIG localize to plasmodesmata and mediate tissue morphogenesis in *Arabidopsis thaliana*. *Development* **141**: 4139–4148.
- Yamaguchi, A., Kobayashi, Y., Goto, K., Abe, M., and Araki, T.** (2005). *TWIN SISTER OF FT (TSF)* acts as a floral pathway integrator redundantly with *FT*. *Plant Cell Physiol.* **46**: 1175–1189.
- Yano, M., Katayose, Y., Ashikari, M., Yamanouchi, U., Monna, L., Fuse, T., Baba, T., Yamamoto, K., Umehara, Y., Nagamura, Y., and Sasaki, T.** (2000). *Hd1*, a major photoperiod sensitivity quantitative trait locus in rice, is closely related to the *Arabidopsis* flowering time gene *CONSTANS*. *Plant Cell* **12**: 2473–2484.
- Zeevaart, J.A.D.** (2006). Florigen coming of age after 70 years. *Plant Cell* **18**: 1783–1789.
- Zeevaart, J.A.D.** (1976). Physiology of flower formation. *Annu. Rev. Plant Physiol.* **27**: 321–348.
- Zhu, Y., Liu, L., Shen, L., and Yu, H.** (2016). NaKR1 regulates long-distance movement of FLOWERING LOCUS T in *Arabidopsis*. *Nat. Plants* **2**: 16075.

OsFTIP1-Mediated Regulation of Florigen Transport in Rice Is Negatively Regulated by the Ubiquitin-Like Domain Kinase OsUbdK γ 4

Shiyong Song, Ying Chen, Lu Liu, Yanwen Wang, Shengjie Bao, Xuan Zhou, Zhi Wei Norman Teo, Chuanzao Mao, Yinbo Gan and Hao Yu

Plant Cell 2017;29;491-507; originally published online March 2, 2017;
DOI 10.1105/tpc.16.00728

This information is current as of October 10, 2020

Supplemental Data	/content/suppl/2017/03/31/tpc.16.00728.DC2.html /content/suppl/2017/03/02/tpc.16.00728.DC1.html
References	This article cites 44 articles, 19 of which can be accessed free at: /content/29/3/491.full.html#ref-list-1
Permissions	https://www.copyright.com/ccc/openurl.do?sid=pd_hw1532298X&issn=1532298X&WT.mc_id=pd_hw1532298X
eTOCs	Sign up for eTOCs at: http://www.plantcell.org/cgi/alerts/ctmain
CiteTrack Alerts	Sign up for CiteTrack Alerts at: http://www.plantcell.org/cgi/alerts/ctmain
Subscription Information	Subscription Information for <i>The Plant Cell</i> and <i>Plant Physiology</i> is available at: http://www.aspb.org/publications/subscriptions.cfm